

# X-ray Monitor Based on Coded-Aperture Imaging for KEKB Upgrade and ILC Damping Ring

J.W. Flanagan, H. Fukuma, S. Hiramatsu,  
H. Ikeda, K. Kanazawa, T. Mitsuhashi,  
J. Urakawa, KEK; G.S. Varner, U. Hawaii;  
J.P. Alexander, M.A. Palmer, Cornell U.

EPAC08, Genoa  
2008.6.24  
TUOCM02

# Summary & Outline

## Summary

We are working on an **x-ray beam size monitor** based on **coded-aperture imaging**, which should permit **broad-spectrum, low-distortion measurements to maximize the observable photon flux per bunch.**

## Outline of talk

- 1) Motivation
- 2) Coded Aperture Imaging Principles
- 3) Design Considerations: diffraction and transmission
- 4) Prototype and test plans

# Motivation

- In considering the possibility of doing low-emittance e-cloud studies for the ILC Damping Ring at the KEKB LER (see MOPP100, this conference), a beam size measurement system with the following requirements was specified:
  - High (few  $\mu\text{m}$ ) resolution.
  - High-speed: bunch-by-bunch readout (2 ns) desired
    - $\Rightarrow$  High flux throughput (wideband, large aperture)
  - Low dependence of magnification on beam current
- These specifications would also be useful for Super KEKB, CESR-TA (ILC-DR study machine), or the ILC DR itself.

# Motivation (cont.)

- KEKB currently uses:
  - SR Interferometers
    - High resolution, but narrow band: no single-bunch measurements
  - Streak cameras, gated cameras:
    - Wideband with reflective optics, but low resolution
- Both systems used at KEKB are also sensitive to mirror distortion due to SR heat load, which introduces beam current dependence to beam size measurements..
- Decided to look into use x-ray monitor.

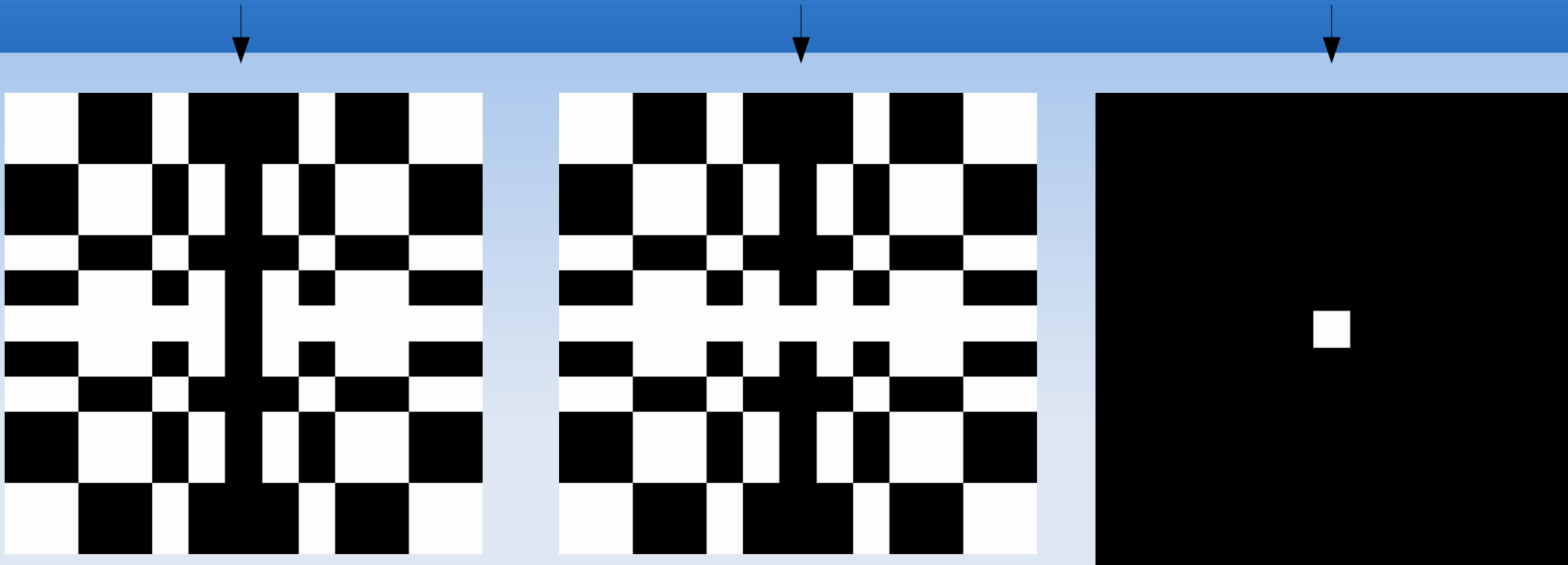
# X-Ray Monitor

- Used or under development at ATF, CESR-TA, Spring-8, PEP-II, elsewhere.
- A Fresnel zone plates is typically used as an X-ray lens
  - Requires the use of a monochromator
    - Sensitive to heat load
      - ==>Beam current dependence
    - Cuts available light level down drastically (1%), necessitating long exposure times
- To maximize bandwidth and minimize number of components, we are considering the use of **coded aperture imaging**.

# Coded Aperture Imaging

- A coded aperture is a mask used to modulate incoming light.
- A pinhole is the simplest type of coded aperture, requiring no monochromator (good), but with very small aperture (bad).
- In 1968 R.H. Dicke (APJL, 153, L101, 1968) proposed the use of a random array of pinholes for X-ray and gamma-ray astronomy. The resulting image needs to be deconvolved back through the mask pattern to reconstruct the source distribution on the sky.
- Improved mask designs were then developed, most notably the Uniformly Redundant Array (URA) mask, which has the nice property that its auto-correlation is a delta function (no sidelobes), and it can achieve open aperture areas of up to 50%.
  - Good overview at: <http://astrophysics.gsfc.nasa.gov/ca>

# Modified URA Mask, Anti-mask, and Cross-correlation



- Image is encoded using mask and decoded using anti-mask, where cross-correlation between mask and anti-mask is delta function.
- Pixel transparency determined by Jacobi function:
  - Is  $(\text{pixel index}) \% \text{DIM} == (i * i) \% \text{DIM}$  for any  $1 < i < \text{DIM}$ ?
    - Yes/No  $\rightarrow$  Open/Closed.
    - 2-D case based on inverse XOR of both indices.
- Note: Fresnel zone plates can in principle also be used as coded apertures. (Barrett, H.H., Horrigan, F.A.: 1973, Appl. Opt., 12, 2686)

# Coded Aperture Decoding

a related version:

In order to perform digital analysis of the picture, Eq. (4) must be quantized. Define  $O(i,j)$  to be an array whose elements represent the number of photons observed during the exposure time in an area equal to that of a single pinhole from a  $\Delta\alpha\Delta\beta$  region of the source centered at  $(i\Delta\alpha, j\Delta\beta, b)$ . Let  $\Delta\alpha = \Delta\beta = c/f$  rad where each pinhole in the aperture is a  $c$  by  $c$  square hole. Define  $A(i,j)$  to be an array with each element denoting the presence or absence of a pinhole in the aperture. If there is a hole at  $(i\cdot c, j\cdot c)$ ,  $A(i,j)$  has the value one, otherwise it is zero. The possible locations for the pinholes are restricted to a grid of discrete points with a spacing equal to  $c$ .

Equation (4) can be approximated to have the same form as Eq. (1):

$$P(k,l) \cong O * A + N \cong \sum_i \sum_j O(i,j)A(i+k, j+l) + N(k,l), \quad (5)$$

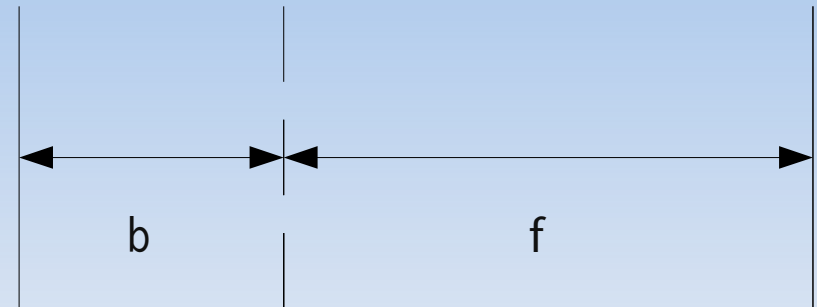
where  $P(k,l)$  should be interpreted as the number of photons received from the object in an  $m\cdot c$  by  $m\cdot c$  area of the detector centered at  $(k\cdot m\cdot c, l\cdot m\cdot c)$  plus some noise  $N(k,l)$ .

The  $P$  array is measured experimentally and since the  $A$  array is known, Eq. (5) is used to determine an estimate of the object intensity distribution. In the correlation analysis methods, the reconstructed object is determined from  $P$  and  $A$  by

$$\hat{O}(i,j) = P * G \cong \sum_k \sum_l P(k,l)G(k+i, l+j), \quad (6)$$

where  $G$  will be chosen such that  $A * G$  is approximately (or exactly) a delta function.

The above is applicable to all coded aperture techniques. We will now employ the above in the implementation of URAs.



Source  
pix. size  
 $= c(b+f)/f$

Mask  
min. hole size  
 $= c$

Detector  
pix. size  
 $= c(b+f)/b$

- Magnification  
 $m=(b+f)/b$

- Fenimore and Cannon, Appl. Optics, V17, No. 3, p. 337 (1978)

# Coded Aperture Imaging (cont.)

- Several reconstruction methods are in use: inversion, cross-correlation, photon tagging (back-projection), Wiener filtering, and iterative methods such as the Maximum Entropy Method and Iterative Removal of Sources (IROS).
- Coded aperture imaging is now a well-established technique in X-ray astronomy, with scattered applications outside that field, e.g.:
  - Medical imaging, thermal neutron imaging, inertial confinement monitoring, and nuclear blast monitoring
- URA masks have been used for the measurement of phase coherence of undulator radiation (J.J.A. Lin et al., PRL 90, 074801), and of an x-ray laser (J. E. Trebes, et al., PRL 68, 588–591 (1992)). The URA was essentially used as a multi-slit interferometer for monochromatic light (not wideband).
- **We believe wideband coded aperture techniques could be useful for general beam profile diagnostics.**

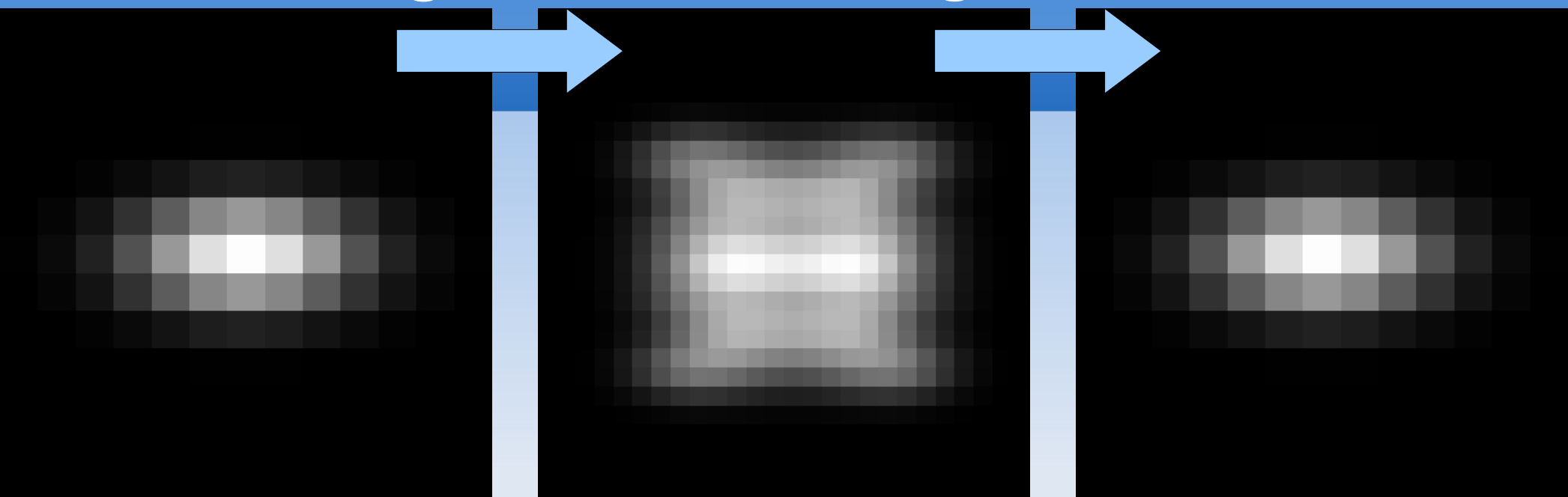
# Examples

- As an illustrative example, here is a simulation of a 13x13 pixel source image, projected through a 13x13 Modified URA mask onto a 26x26 CCD.
  - The image represents a beam with  $\sigma_y=5 \mu\text{m}$  (typical of ILC Damping Ring study mode, or SuperB super-low emittance mode) and  $\sigma_x=10\mu\text{m}$ , with minimum mask pinholes  $4 \mu\text{m}$  on a side.
  - With a 5:1 magnification factor (e.g., mask 6 meters downstream of source, and CCD 24 meters downstream of mask), the CCD pixels would be  $25 \mu\text{m}$  on a side, which is about the size of the x-ray CCD in use at the ATF. The source resolution elements would be  $5 \mu\text{m}$  on a side.
- The reconstruction method used is direct decoding.
- In the second case, a random scattering of 10% noise has been added to the CCD image, which has then been reconstructed via decoding.

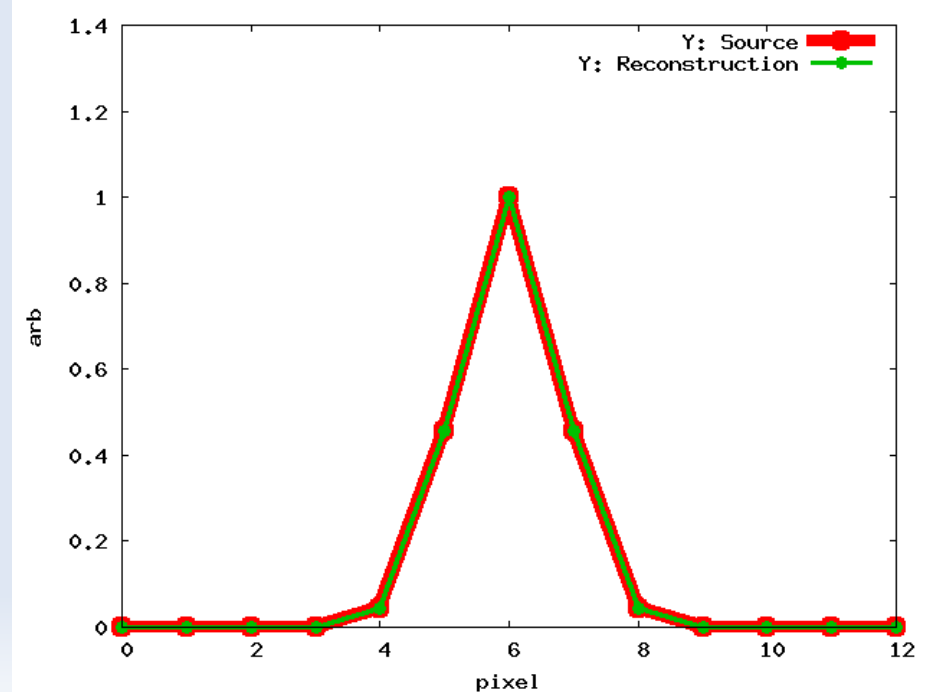
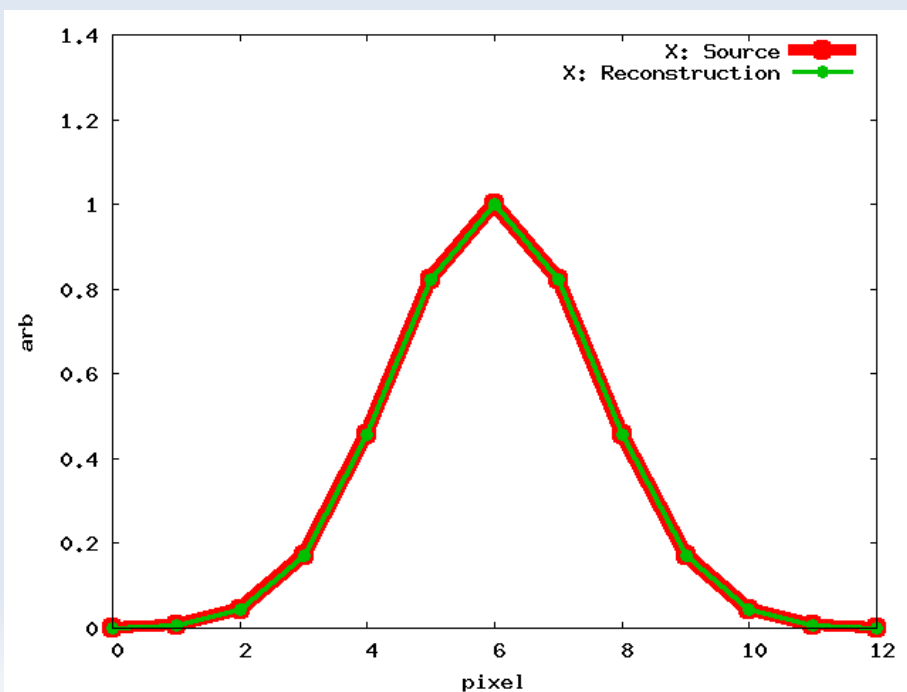
# Source Image

# Detector Image

# Reconstruction



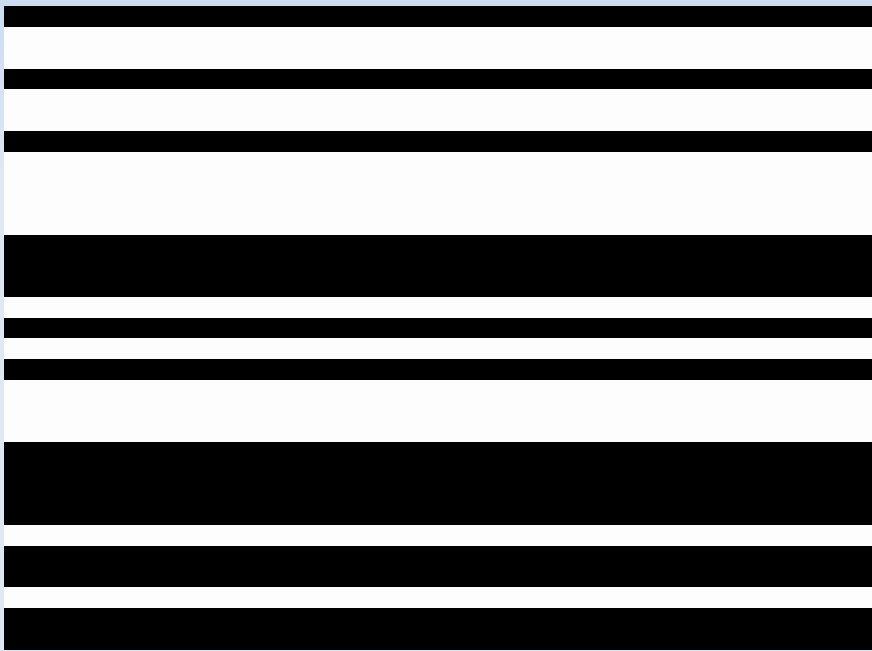
## Reconstructed Horizontal and Vertical Profiles



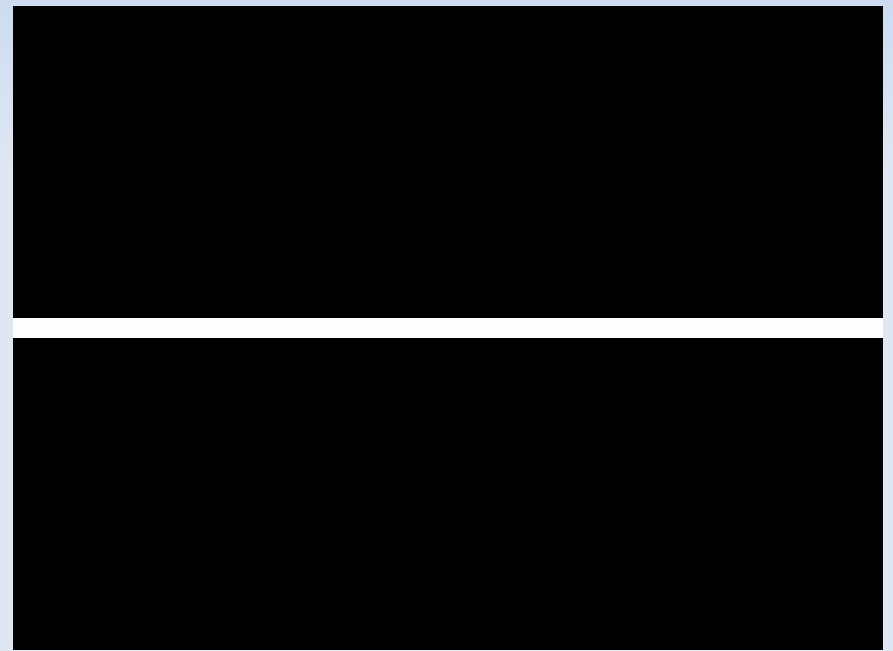


# Vertical-only mask: 1x31

Much faster reconstruction when using iterative methods (1-D vs 2-D problem)

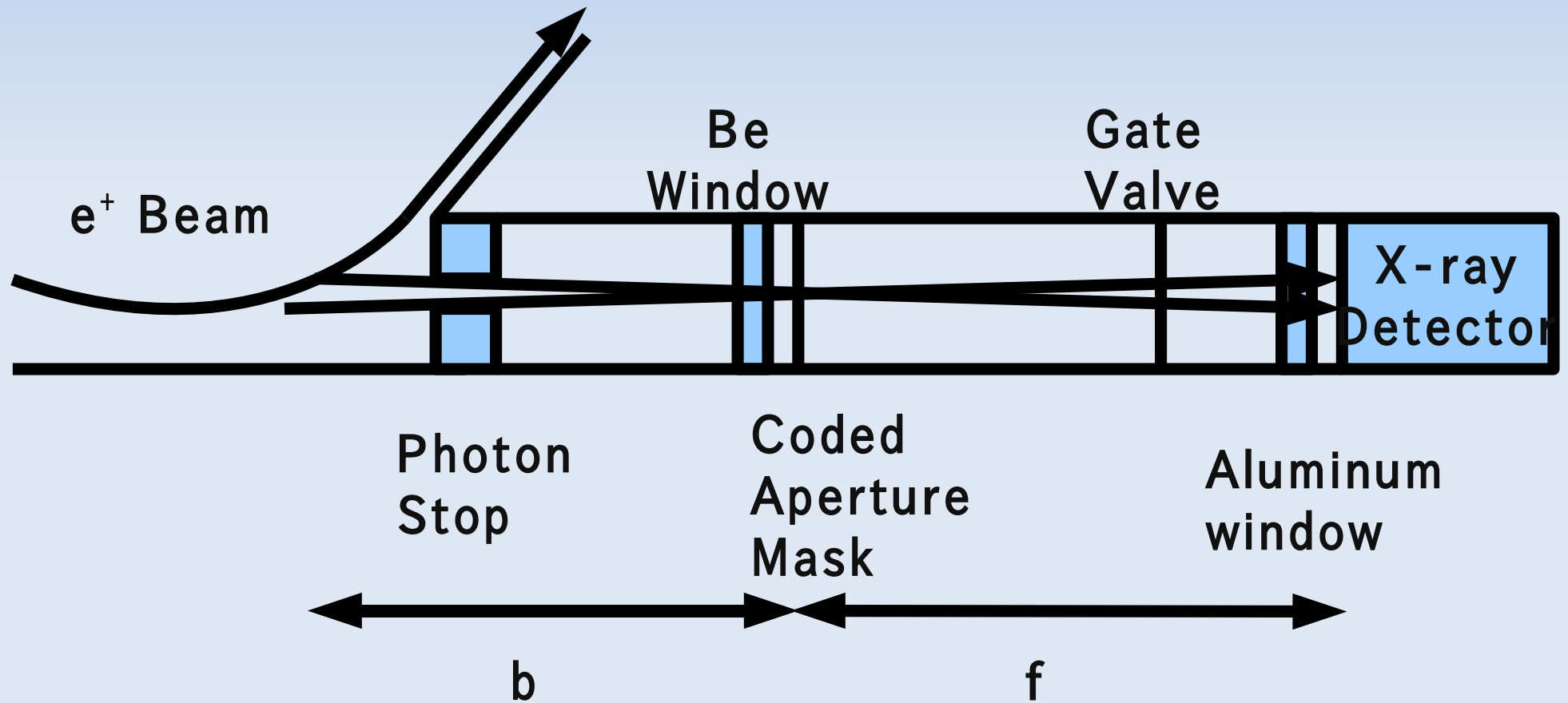


1-D URA Mask

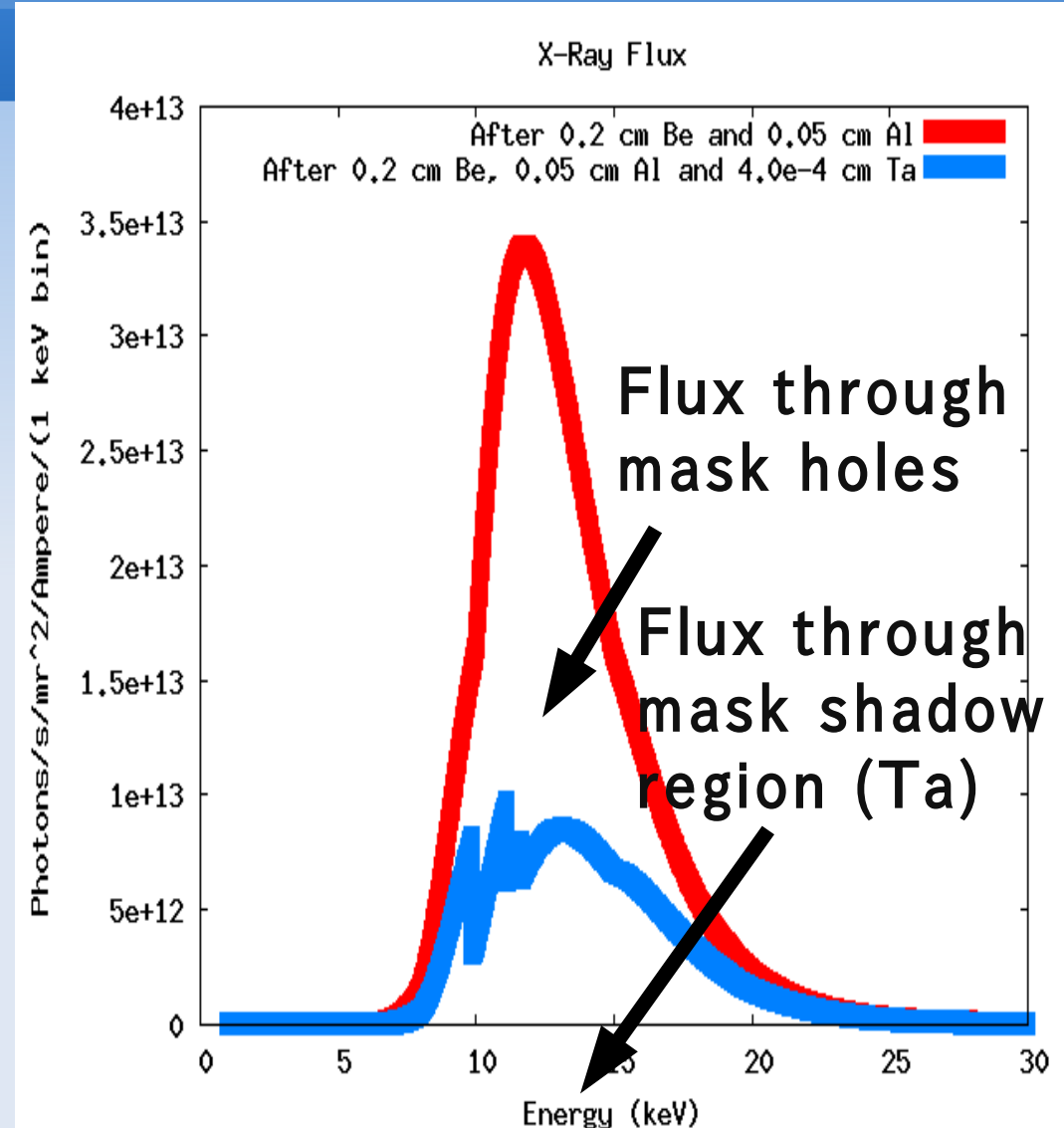
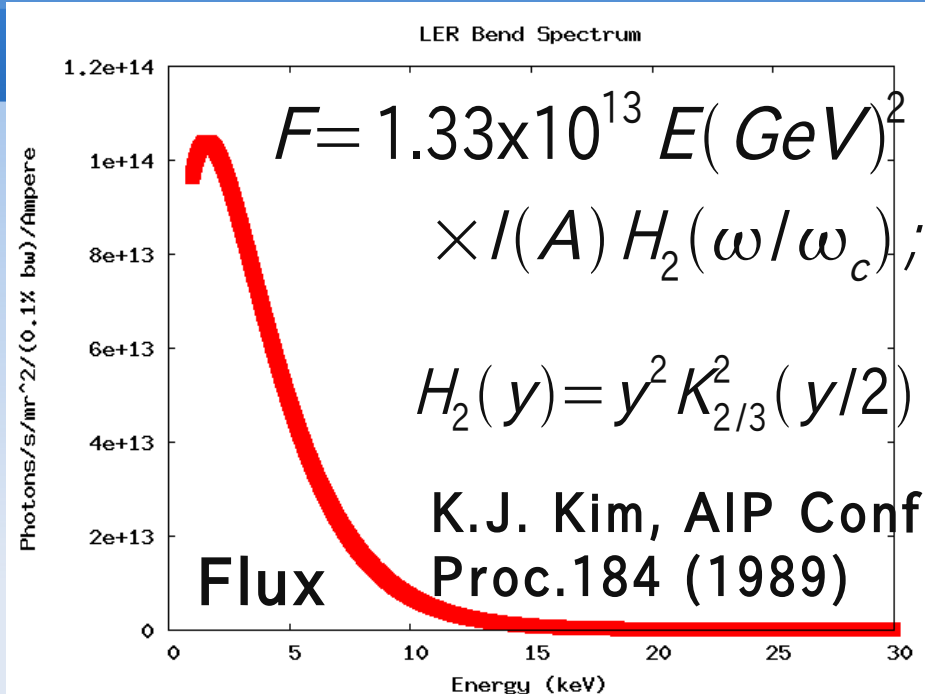


Autocorrelation

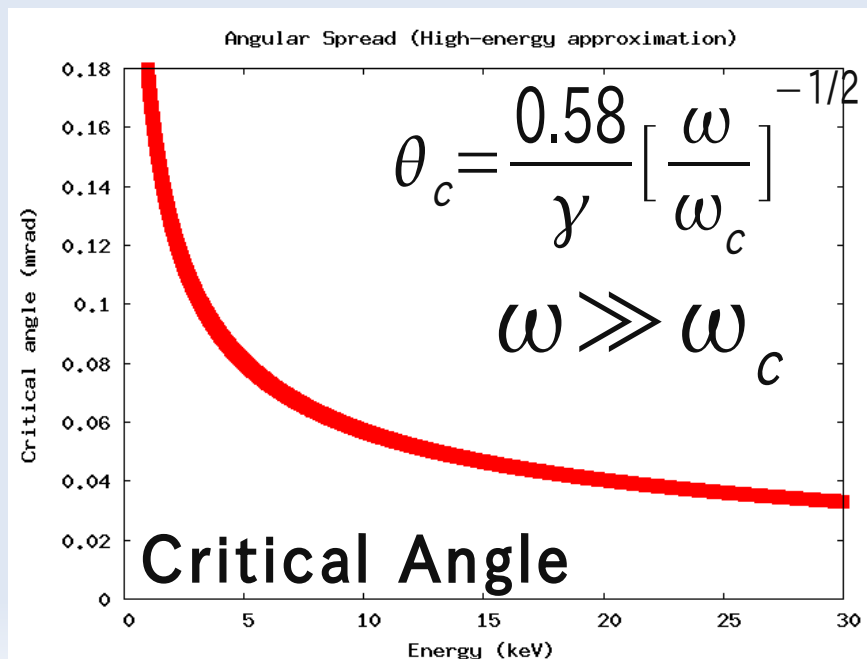
# Schematic Layout



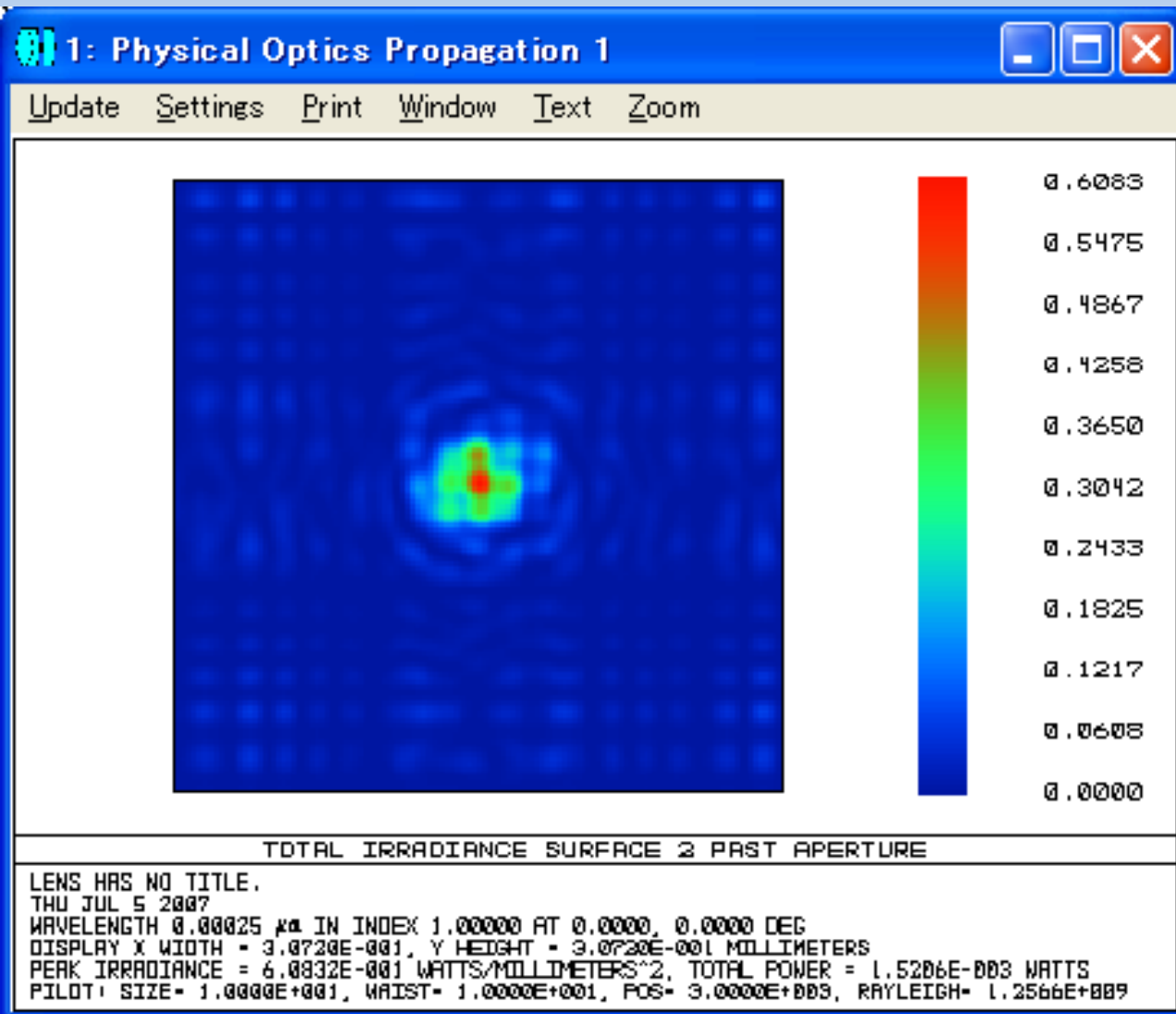
# X-Ray Flux for KEKB in ILCDR study mode



Signal 1626.2 photons/turn/mA  
Background 566.748 photons/turn/mA



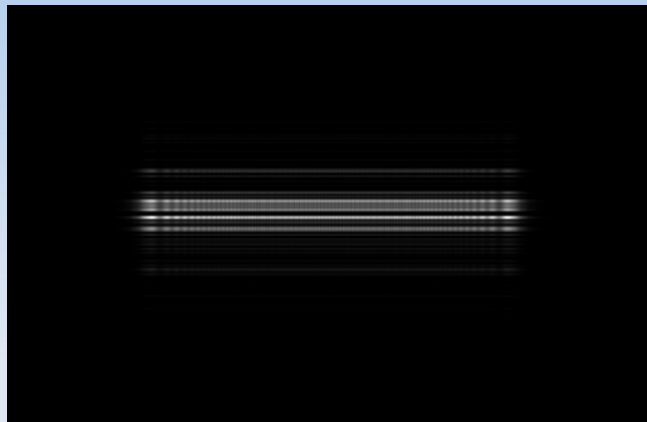
# But, diffraction cannot be ignored



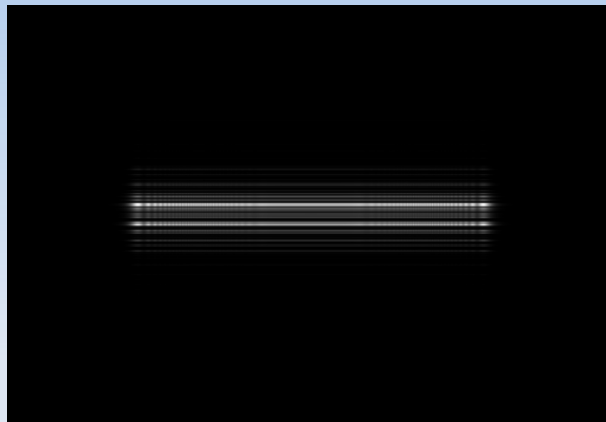
- x-ray: 5 keV
- URA mask: 23x23
- Hole size: 2.4  $\mu\text{m}$
- Distance from mask to camera: 3 m
- Diffraction calculated using Zemax
- This can in principle still be reconstructed if we know the spectrum, using **iterative methods** such as maximum entropy.

# Vertical-only mask: 1x31, 4 um min. aperture

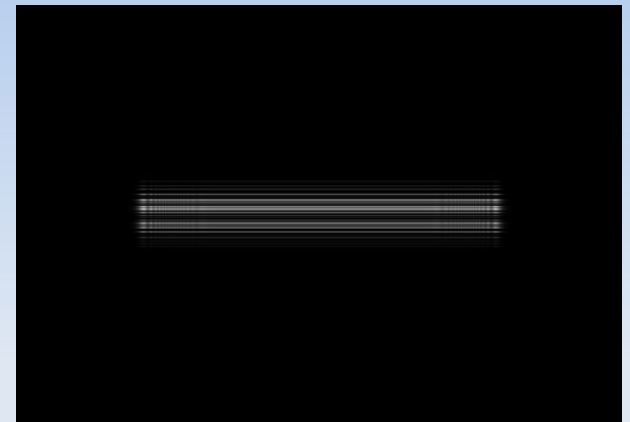
Irradiance as function of photon energy. Mask->detector = 24 m



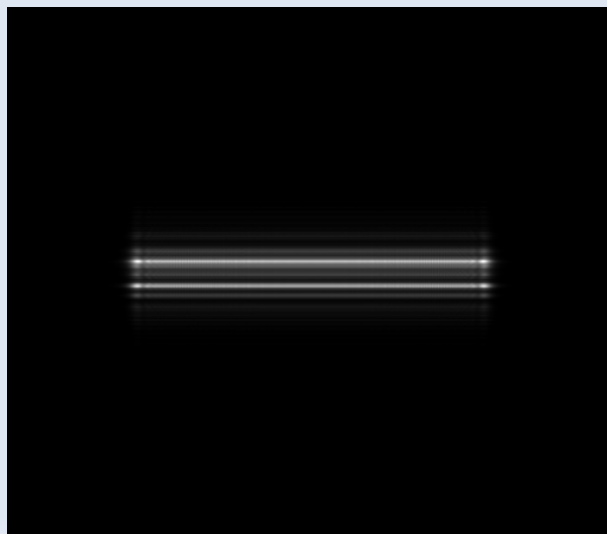
6.2 keV



12.4 keV

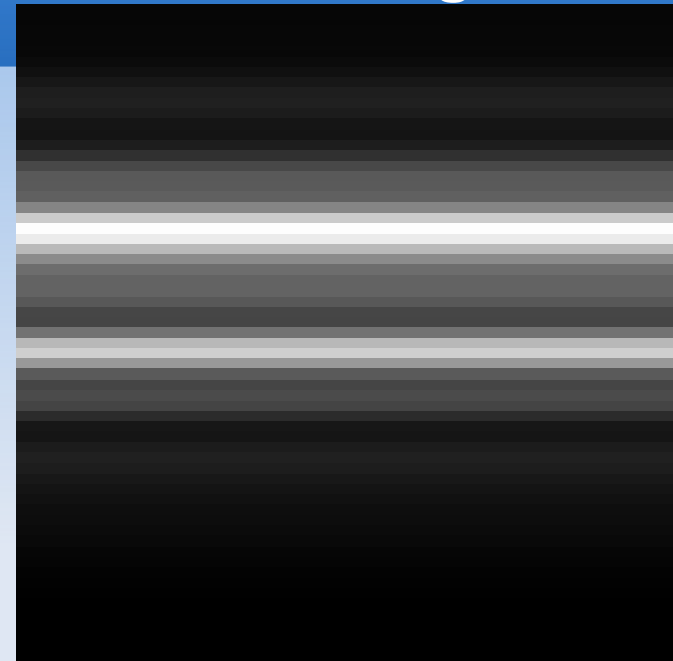
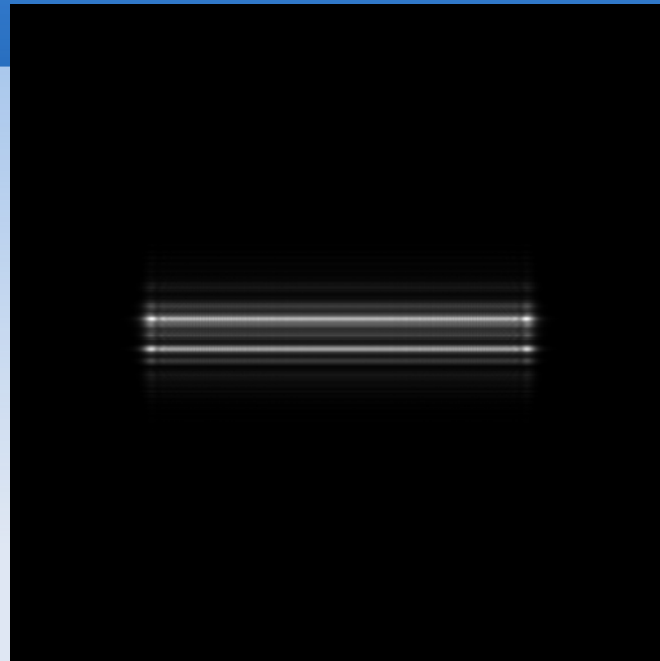
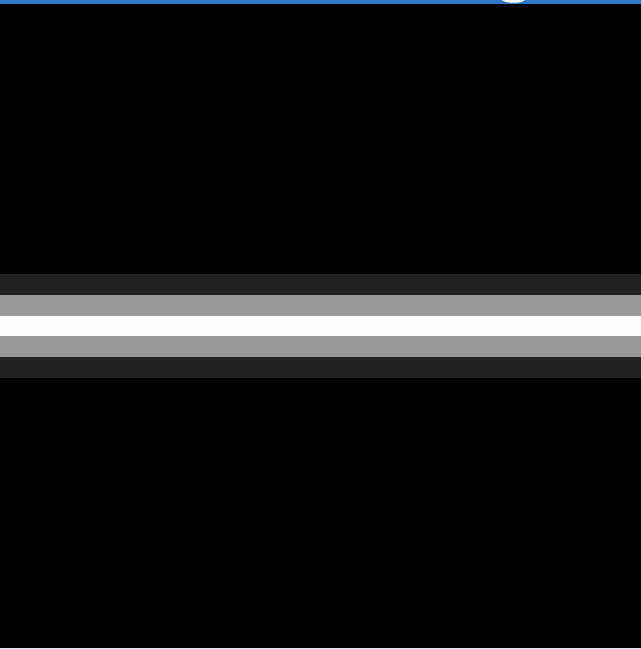


24.8 keV

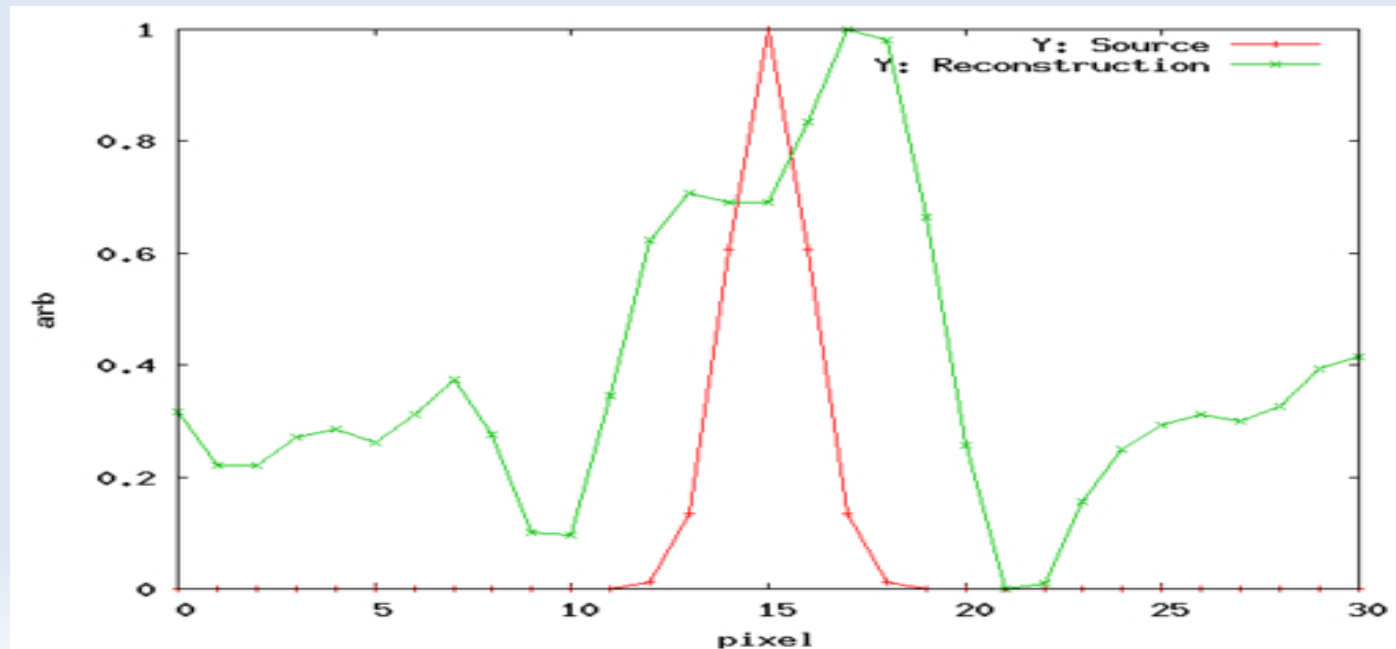
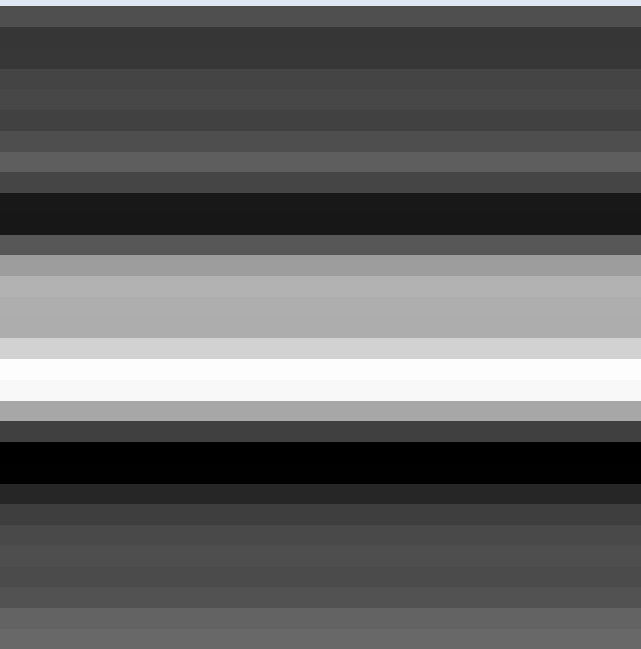


Averaged over spectrum

URA 1x31 x 4 um; Decoding; Beam sigy=5 um, spec. 5-30 keV; No Noise  
Source Image      Mask Irradiance w/diffraction      CCD Image

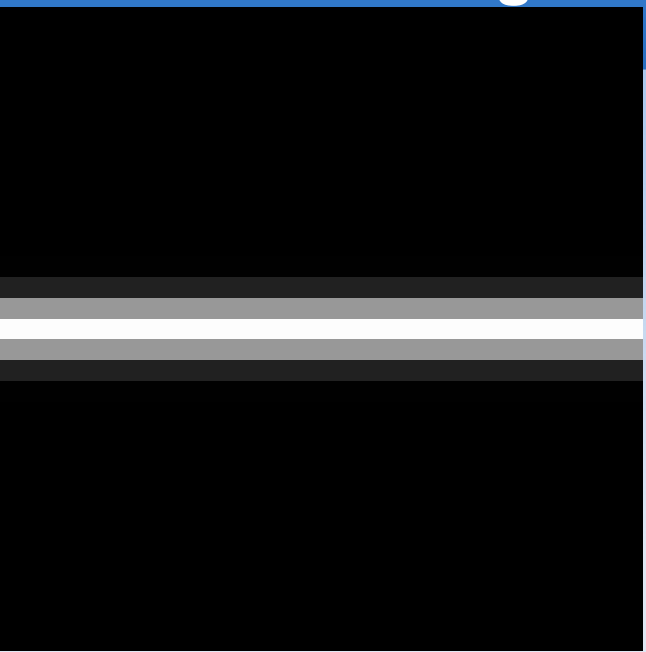


## Reconstructed Image and Profile

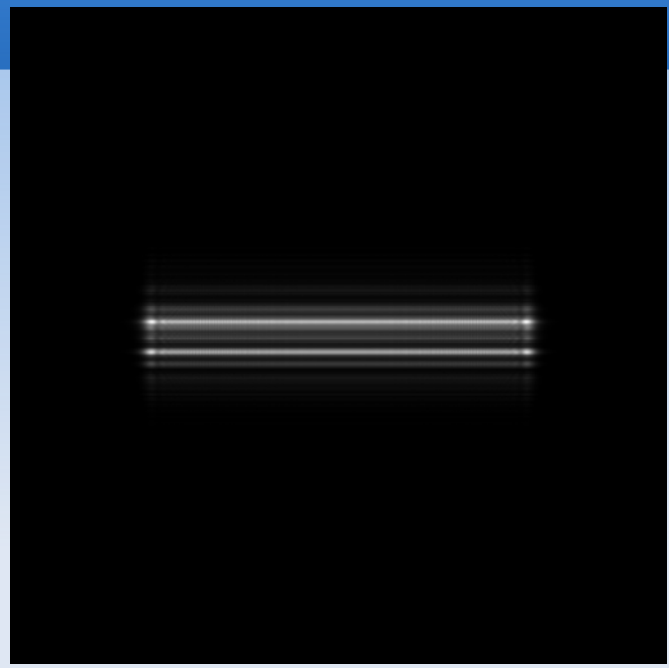


URA 1x31 x 4 um; Max. Ent. reconstruction; Beam sigy=5 um, 5-30 keV; No Noise

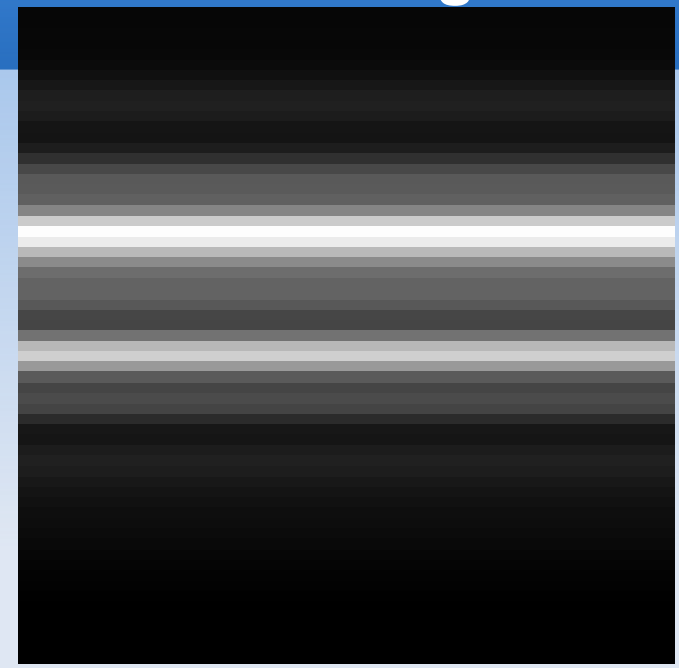
Source Image



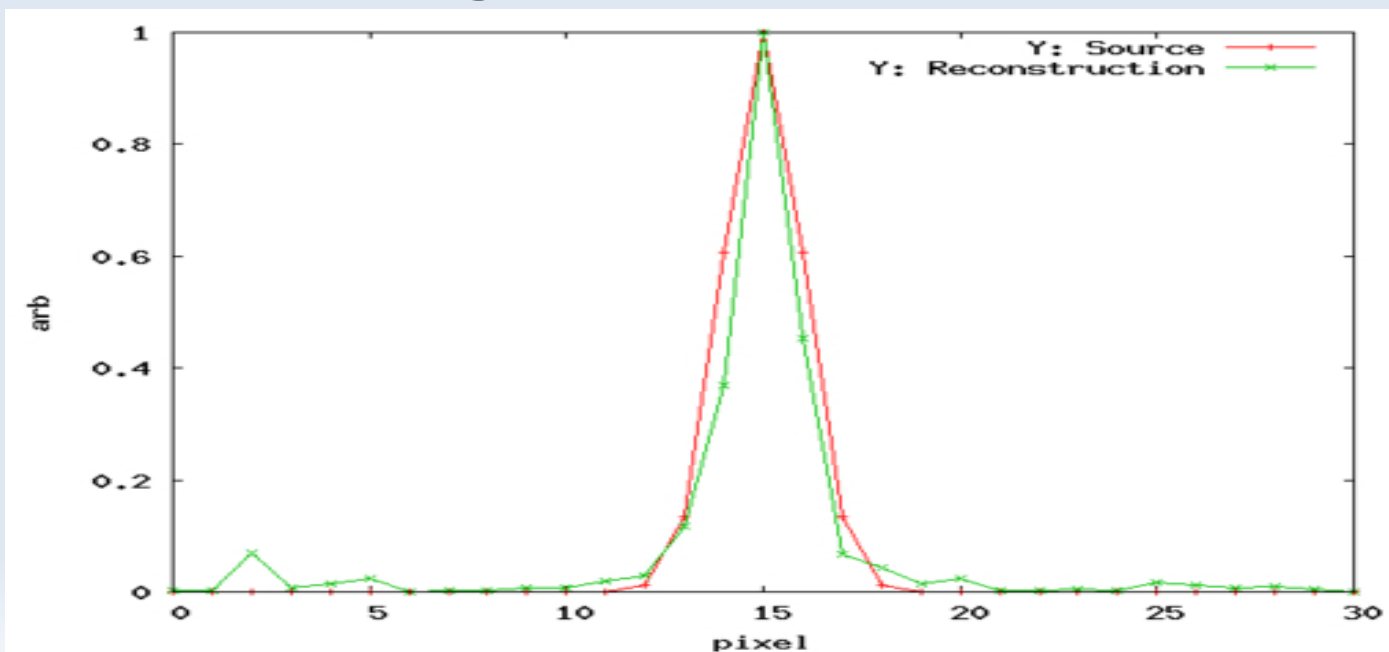
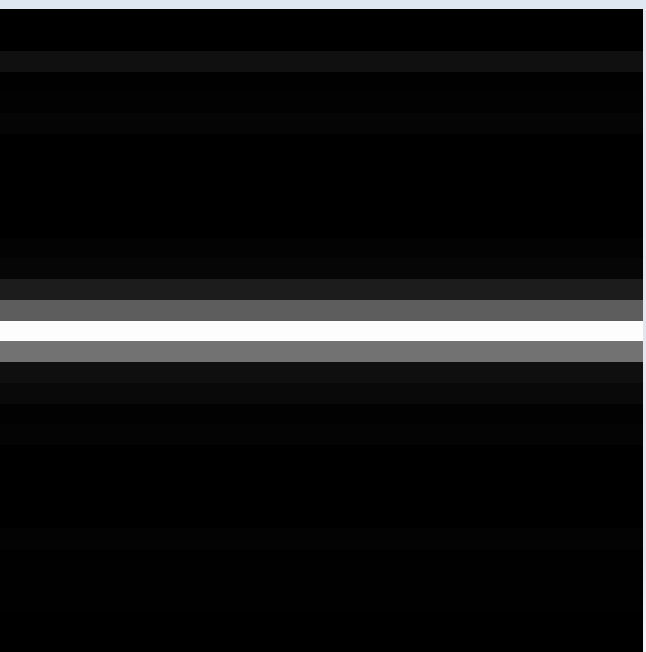
Mask Irradiance w/diffraction



CCD Image

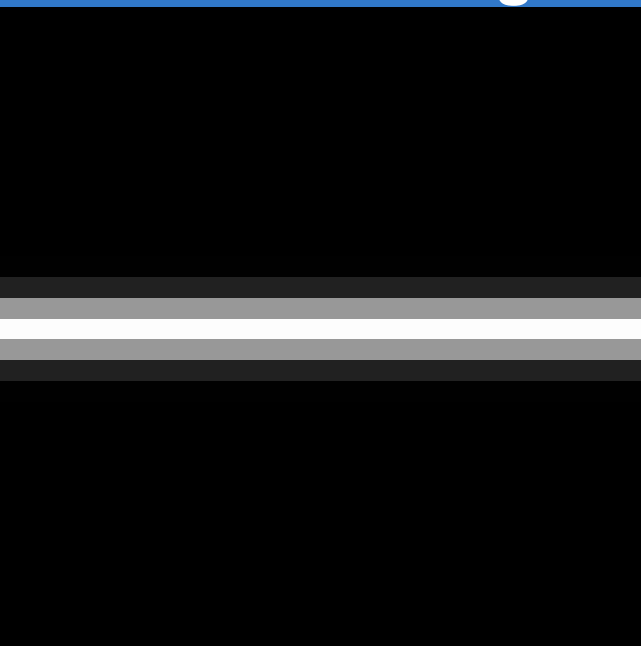


## Reconstructed Image and Profile

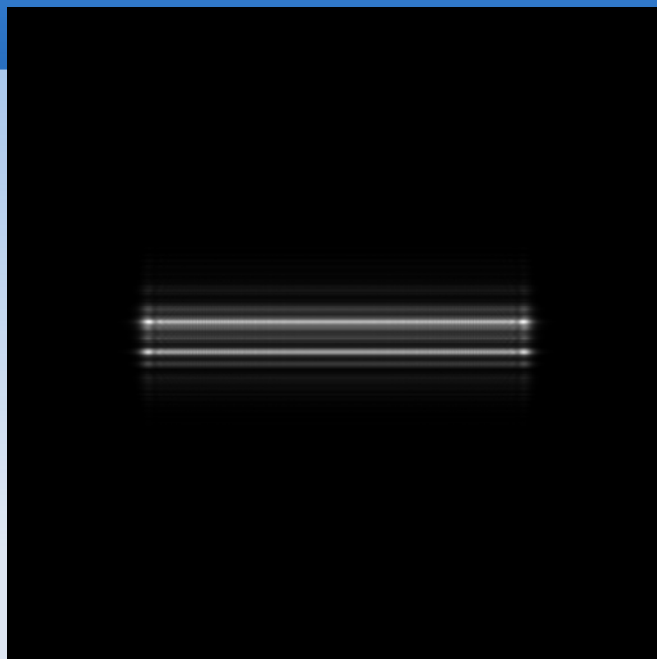


URA 1x31 x 4 um; Iterative reconstruct.; Beam sigy=5 um, 5-30 keV; 10% Noise

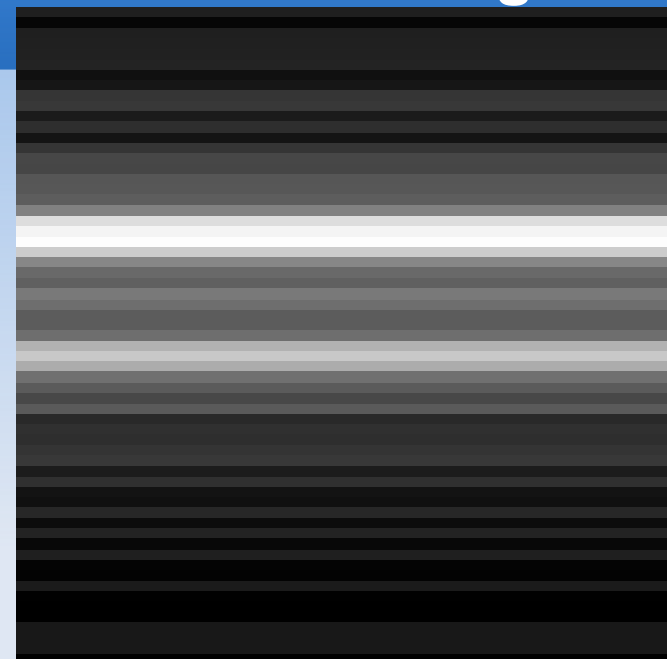
Source Image



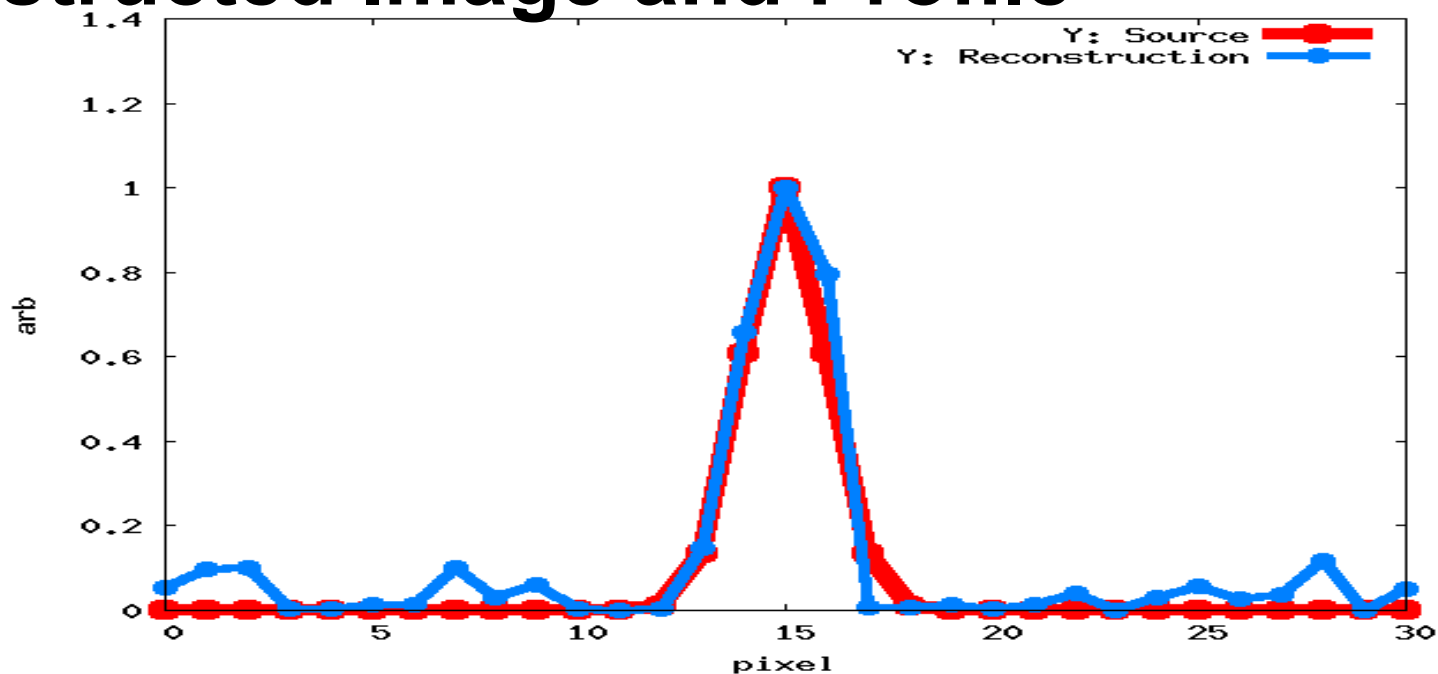
Mask Irradiance w/diffraction



Detector Image



## Reconstructed Image and Profile



# Index of refraction also cannot be ignored

$$n = (1 - \delta) + i\beta$$

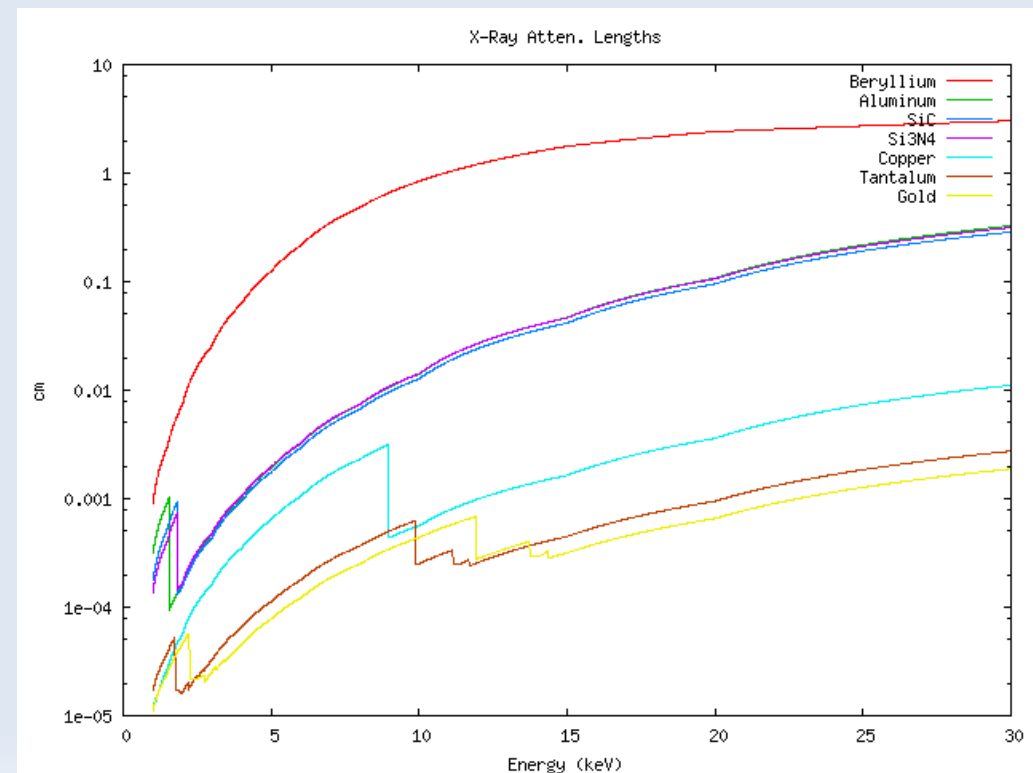


Phase shift

- At high energies the transmission and phase shift through mask region becomes significant.



Attenuation

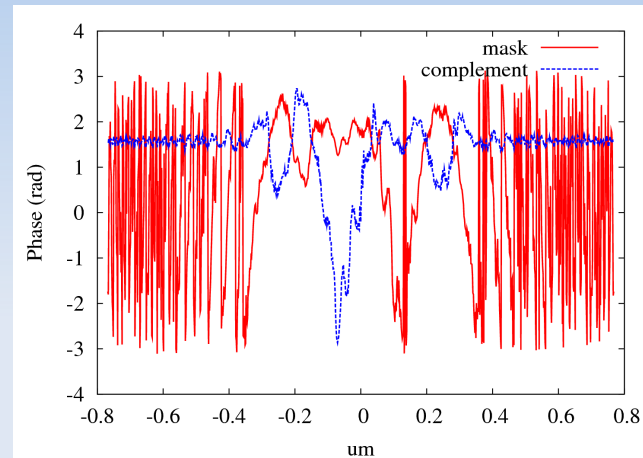
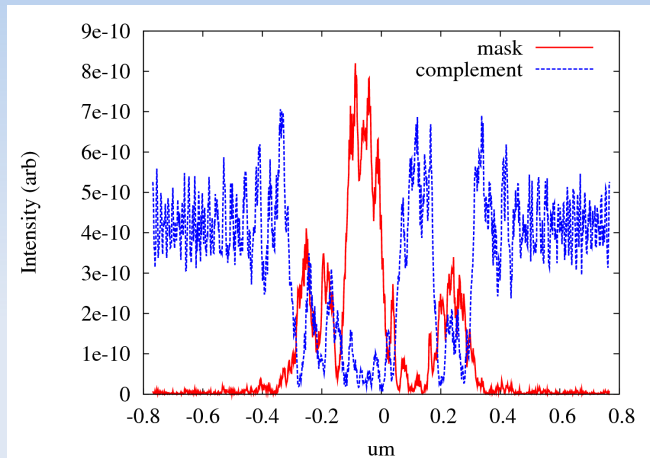


# Simulation Including Transmission/Refraction



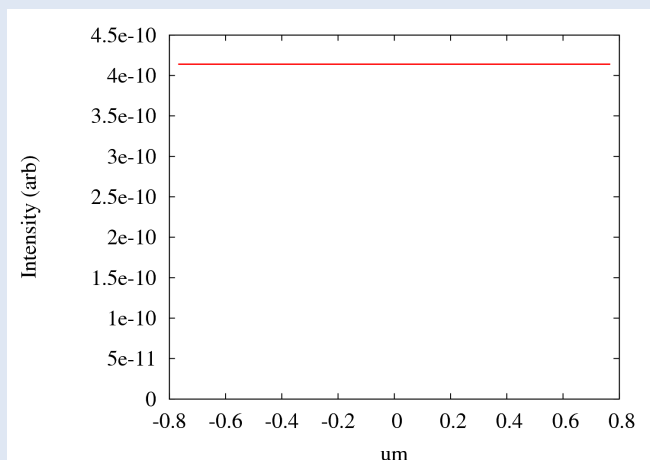
Example @ 0.1 A (1.2 keV)

- At each wavelength, calculate effective mask pattern from phase and amplitude data of mask and complementary mask, apply attenuation and phase shift from mask material, then add vectorially

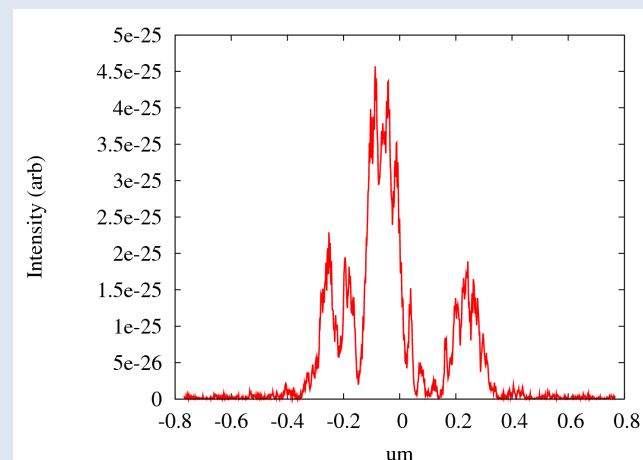


Mask & Complement Intensity

Mask & Complement Phase



Simple Vector Sum Intensity  
(Babinet check)



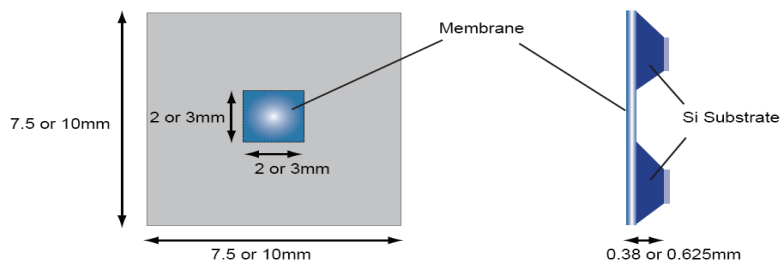
4 um Ta Mask Intensity

- Zemax (commercial program) used for wavefront calculations.
- Do weighted sum over relevant wavelength range to get **effective mask pattern**.

# Prototype Tests at CESR-TA



- Started testing of prototype mask at CESR-TA
  - 4  $\mu\text{m}$  Ta mask made by NTT-AT
- Using CHESS user beamlines, can observe 2.1-5.3 GeV beams.
- Vertical beam sizes from 30-150  $\mu\text{m}$ , eventually down to  $\sim 10$   $\mu\text{m}$  at low energy.

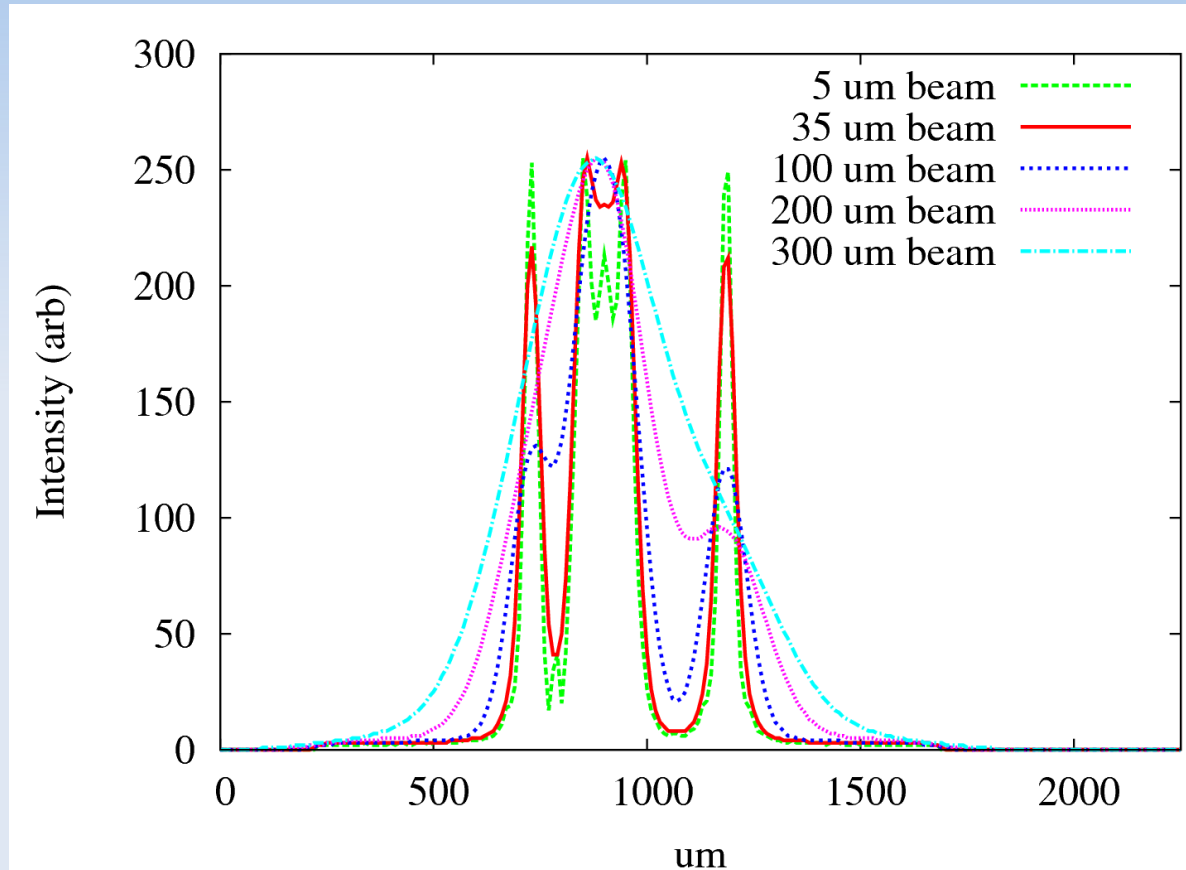
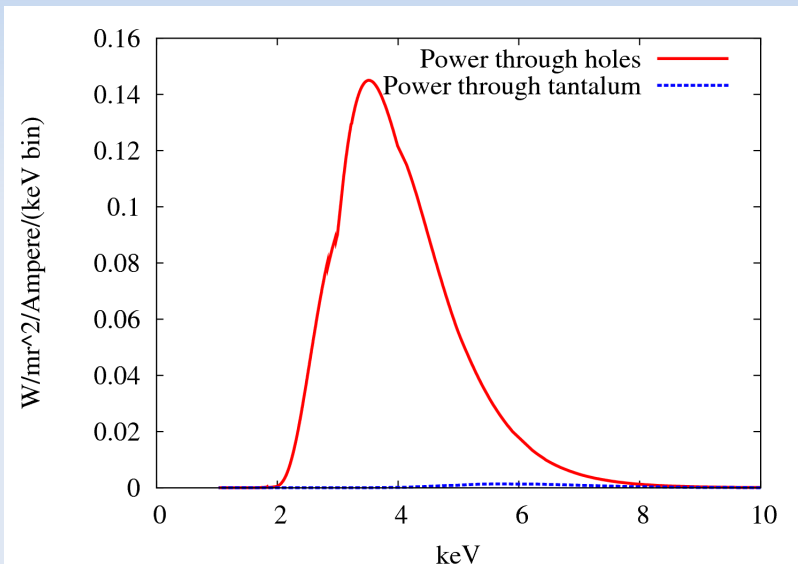


Schematic of Membrane

Remarks:  
The specifications stated in this brochure are representative values and not guaranteed. Also, please kindly note that the specifications may change without prior notice for product update.

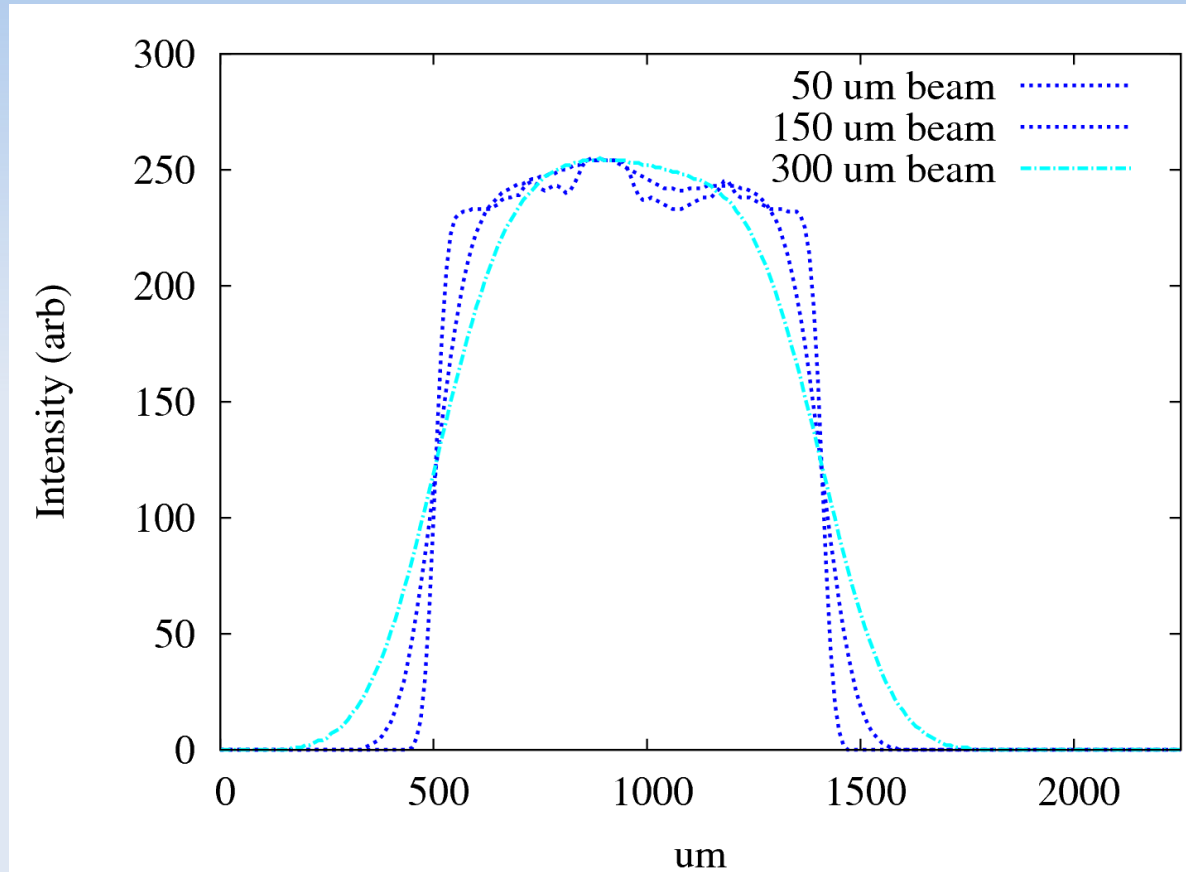
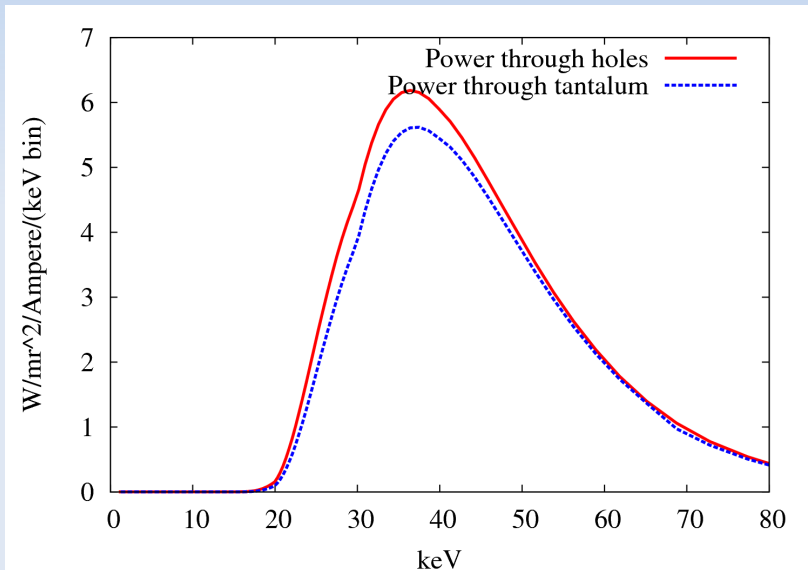
NTT Advanced Technology Corporation  
International Sales and Marketing Department  
Musashino Center Building 6F, 1-19-18, Naka-cho,  
Musashino-shi, Tokyo, 180-0011, Japan  
TEL : +81 422 36 6715  
FAX : +81 422 36 6702  
E-mail : [moreinfo@ntt-at.co.jp](mailto:moreinfo@ntt-at.co.jp)  
URL : <http://www.ntt-at.com>

# Prototype testing at CESR-TA



- X-ray spectrum, and simulated detection pattern for CESR-TA at **2.1 GeV**.

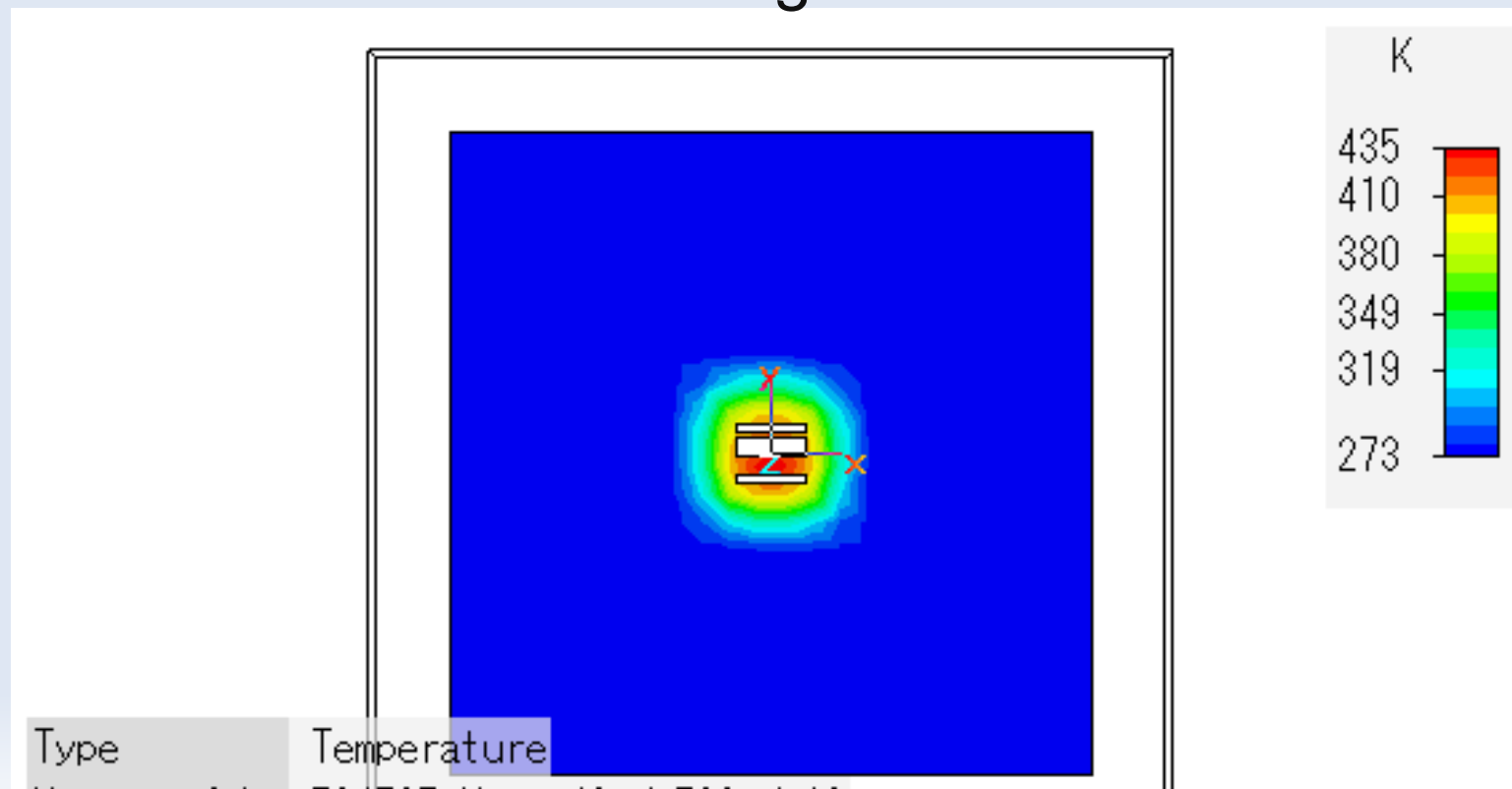
# Prototype testing at CESR-TA



- Xray spectrum, and simulated detection pattern for CESR-TA at **5.3 GeV**.

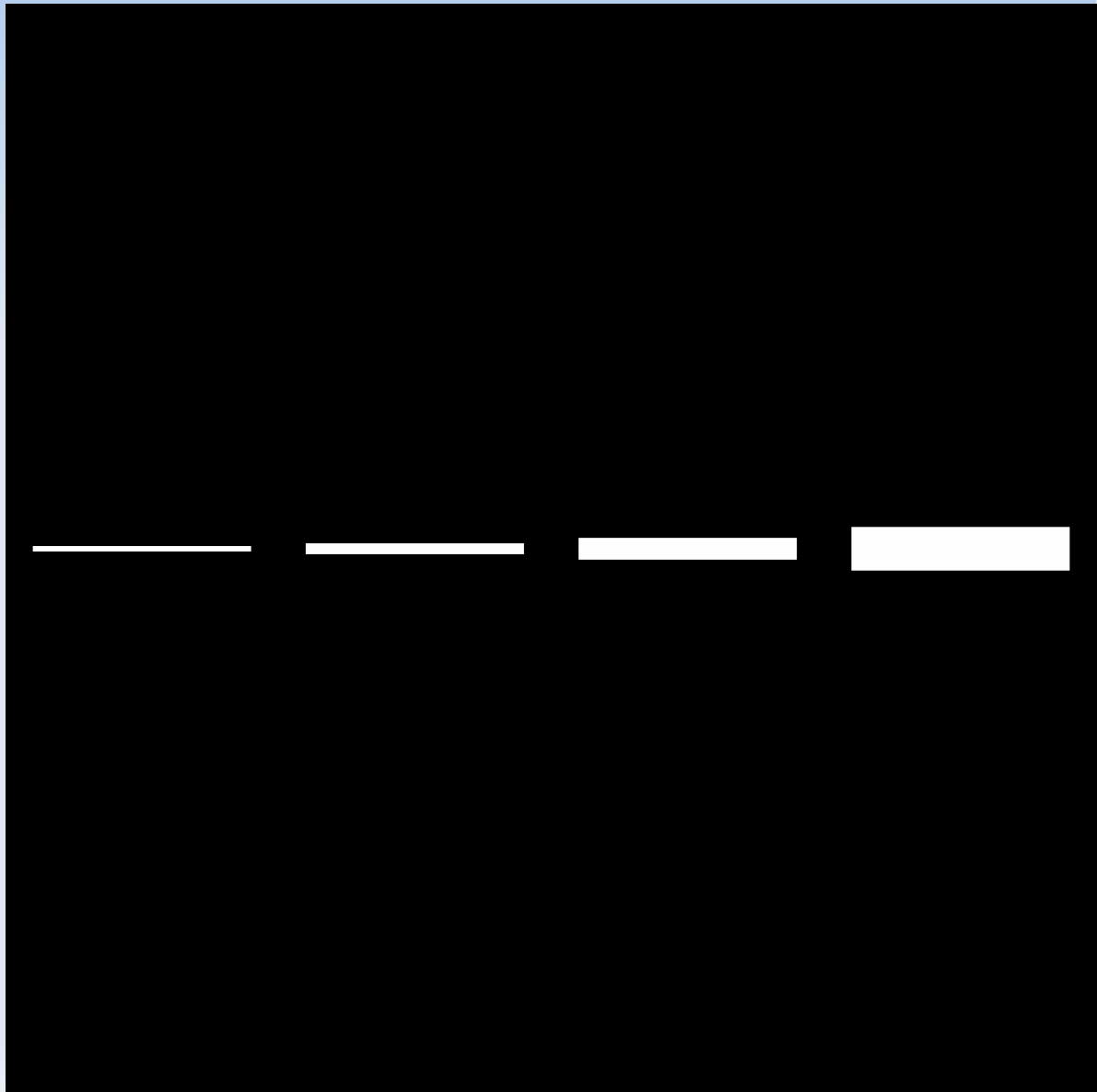
# Heat Load

- Calculated heat load due to X-radiation absorbed in tantalum not a problem at 2.1 GeV.
- At 5.3 GeV, Al filter needed to cut down heat load to manageable levels.
  - Si backplane in mask region would help at high-energy, but would be too absorbing at 2.1 GeV.



# Other tests: simulation verification

- Test slit pattern fabricated
- Varying slit widths from 5-40  $\mu\text{m}$
- Will test with narrow-band x-ray beam to verify simulated response function in detail.



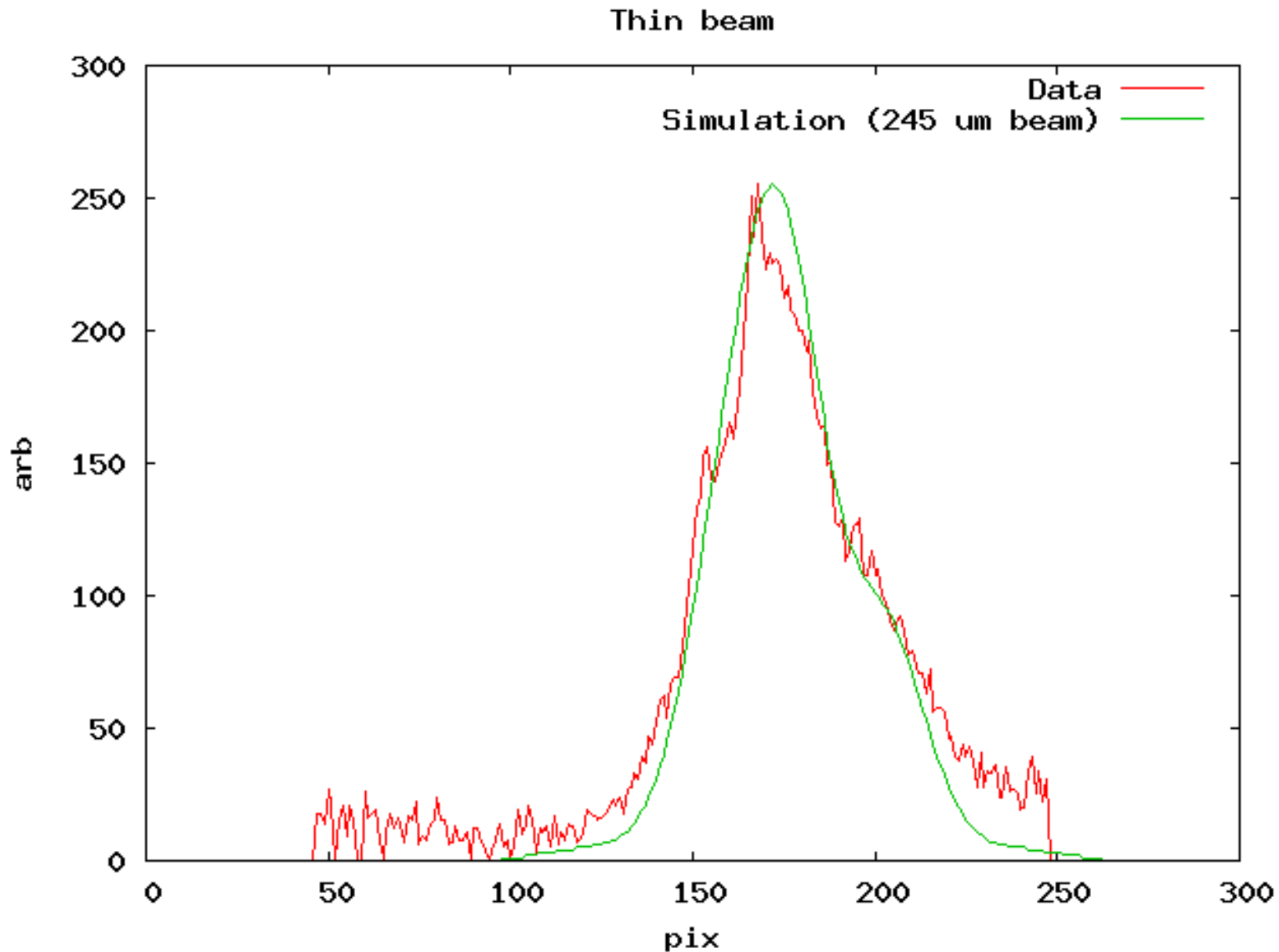
# Conclusion

- Coded Aperture Imaging seems to hold promise for x-ray beam profile and position monitoring.
- Appropriate mask pattern, construction, and reconstruction method need to be considered for each situation.
  - URA pattern allows very fast reconstruction when diffraction is not an issue. Otherwise, iterative methods are required.
- But in principle, a relatively simple, robust system might be able to be constructed from a photon with aperture and beryllium window in the beam pipe at a source bend, a mask, and an x-ray pixel sensor, plus filtering (Al, e.g.) as needed to reduce power (at expense of flux).
- Status:
  - Prototype mask has been constructed, and has begun testing using wide spectrum beam at CESR-TA. Narrow-band tests planned to validate simulated diffraction in detail.
  - Work on detector and readout system development also underway at Cornell and U. Hawaii.

**Extras**

# First Glance

## Very Preliminary!

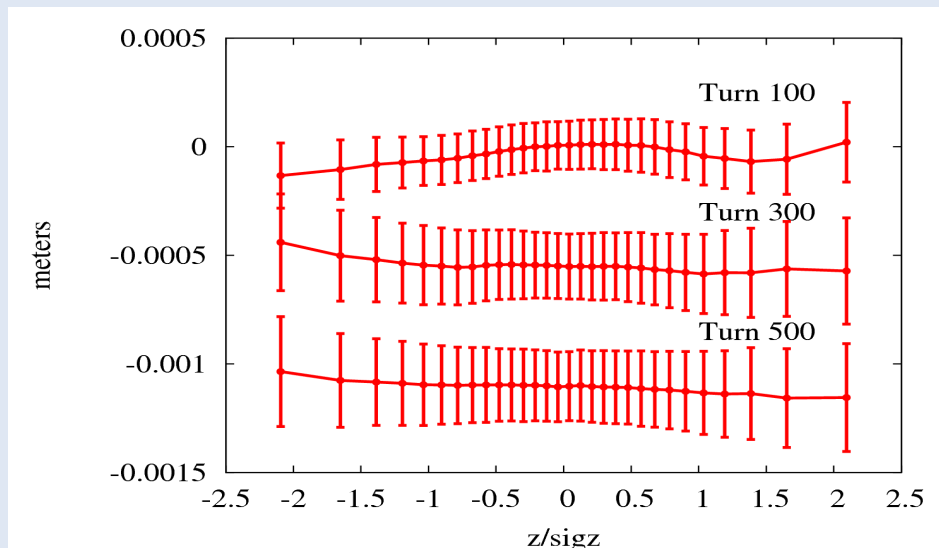


# Detector & Readout

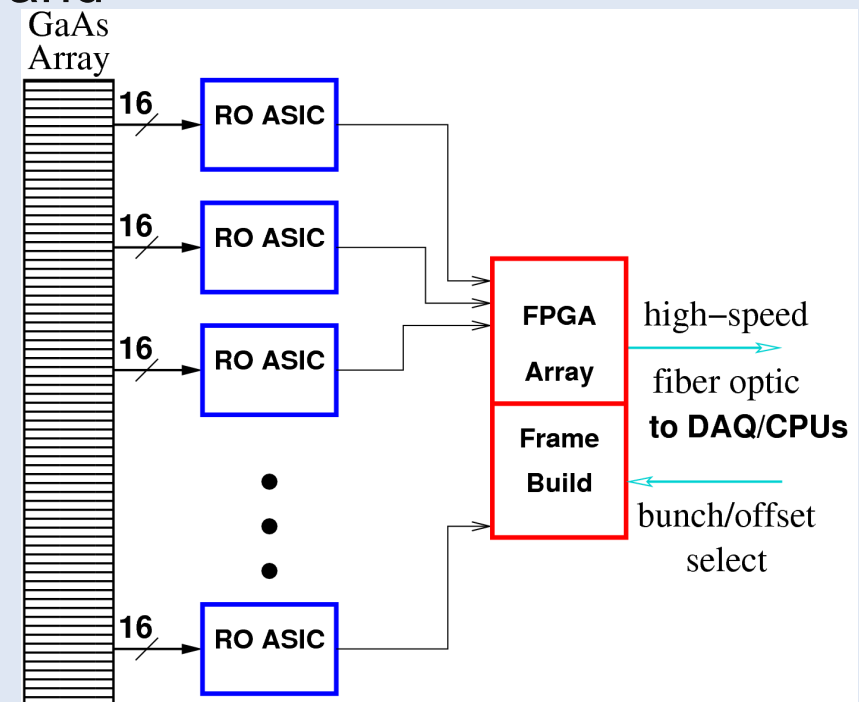
- Detector and bunch-by-bunch readout have been under development at Cornell from previously.
- A future readout design at UH aims for 6 GS/s initially (interleaved) using high-speed sampling ASICs.
  - Ultimate goal (dream?): read out head and tail of bunch separately.

表 1: Specifications for the image array readout ASIC and system.

ASIC:	
Sampling rate	16 ch. at 32 GSa/s (interleaved 6 GSa/s)
Samples/chan.	64
Conversion/ readout time	< 10 $\mu$ s
Resolution	9 bit
Data rate	205 MB/s
System:	
No. of ASICs	16 (512 ch.)
Data rate	3.3 GB/s



E-cloud induced head-tail motion simulation, adapted from E. Benedetto *et al*, PAC07, 4033 (2007)



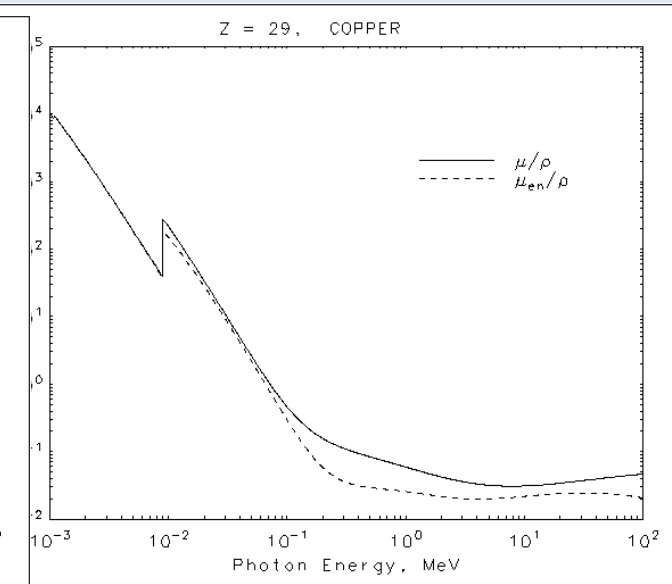
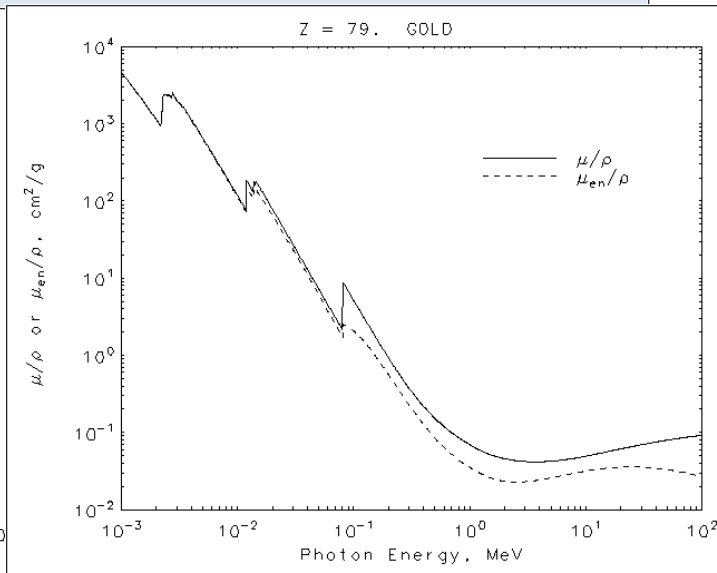
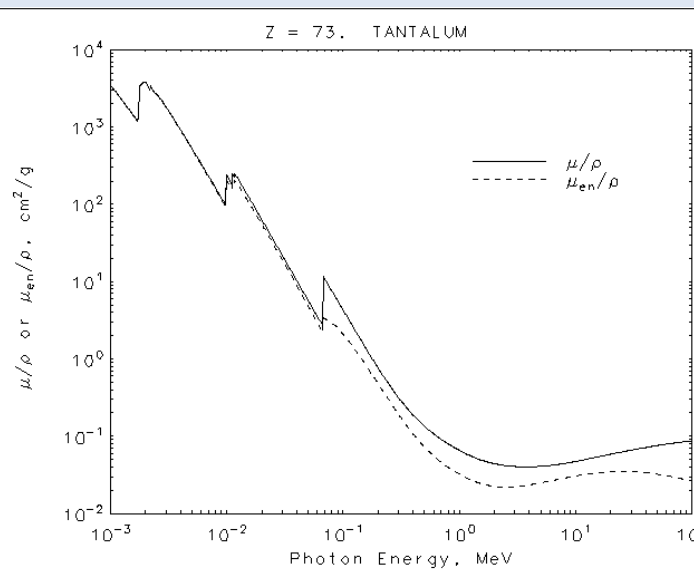
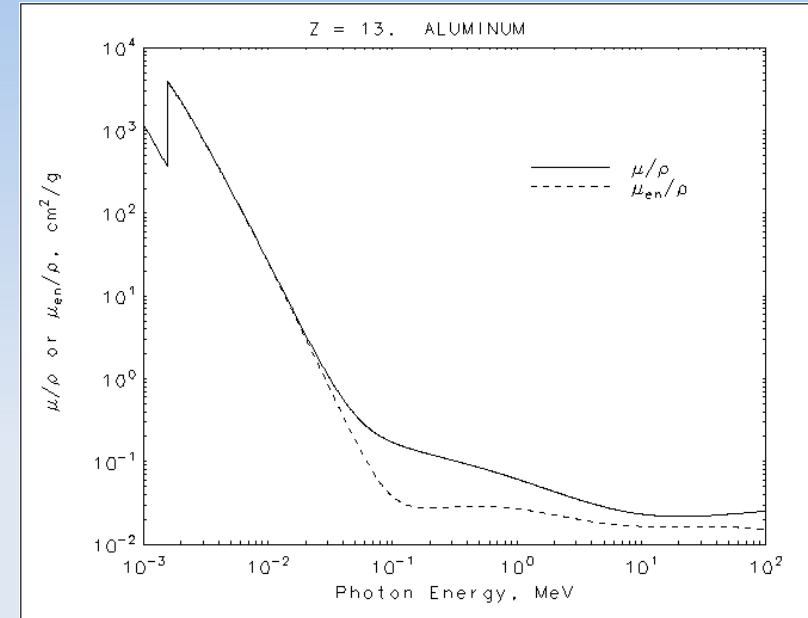
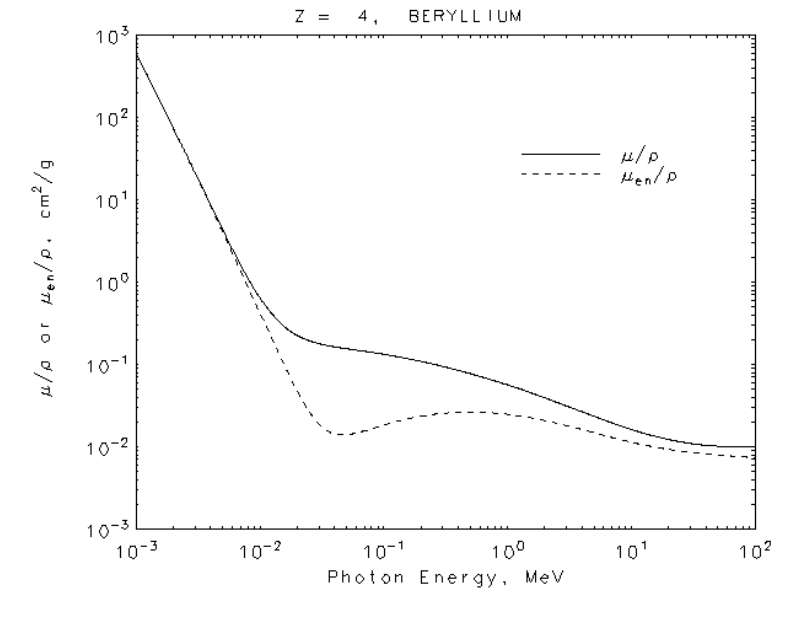
Specs. & Diagram: G. Varner

# Detector & Readout (cont.)

- Detector: J. Alexander and M. Palmer have been testing Hamamatsu G9494-512 InGaAs photodiode array, which has a 25  $\mu\text{m}$  pixel pitch and 30-35 ps rise/fall times, but without the Hamamatsu-provided video readout backend, which is too slow for bunch monitoring purposes.
  - A similar device from Kyosemi is also under consideration.
- A 1000-element, 25  $\mu\text{m}$  pitch GaAs sensor array is also being constructed by LightSpin, Inc., and should be available for testing soon. (G. Varner)
- To minimize capacitance and readout time, an integrated detector and digitizer on one chip may ultimately be needed. Initially however, we will pursue detector investigation and ADC development using a separate array, then work towards an integrated system.

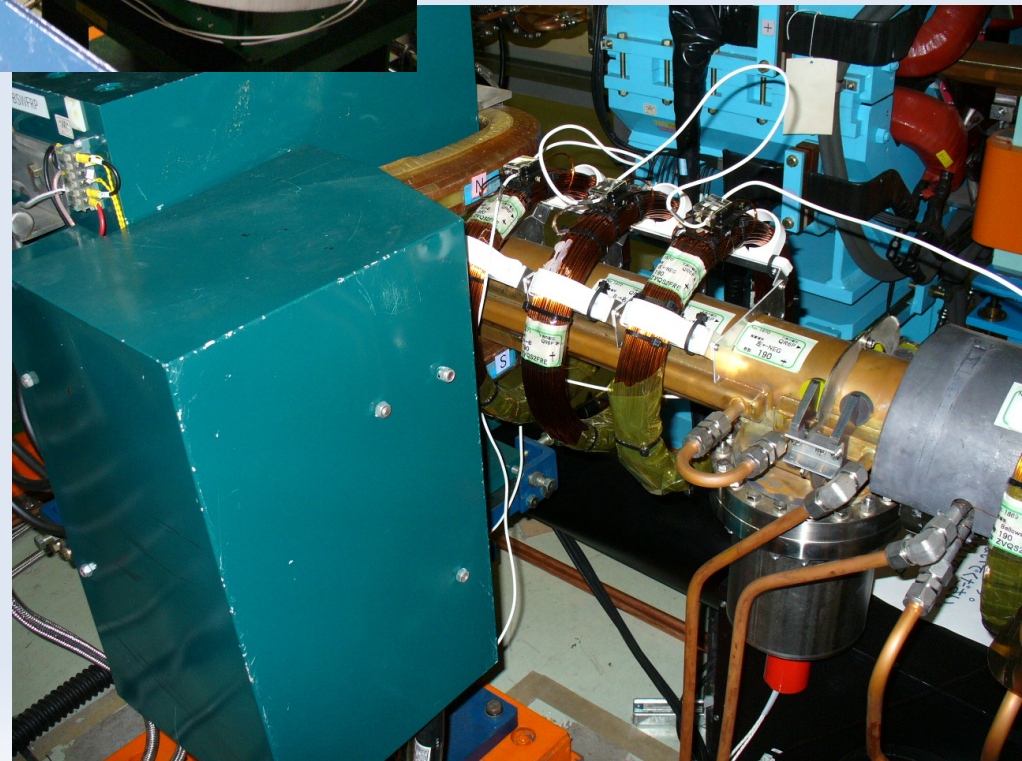
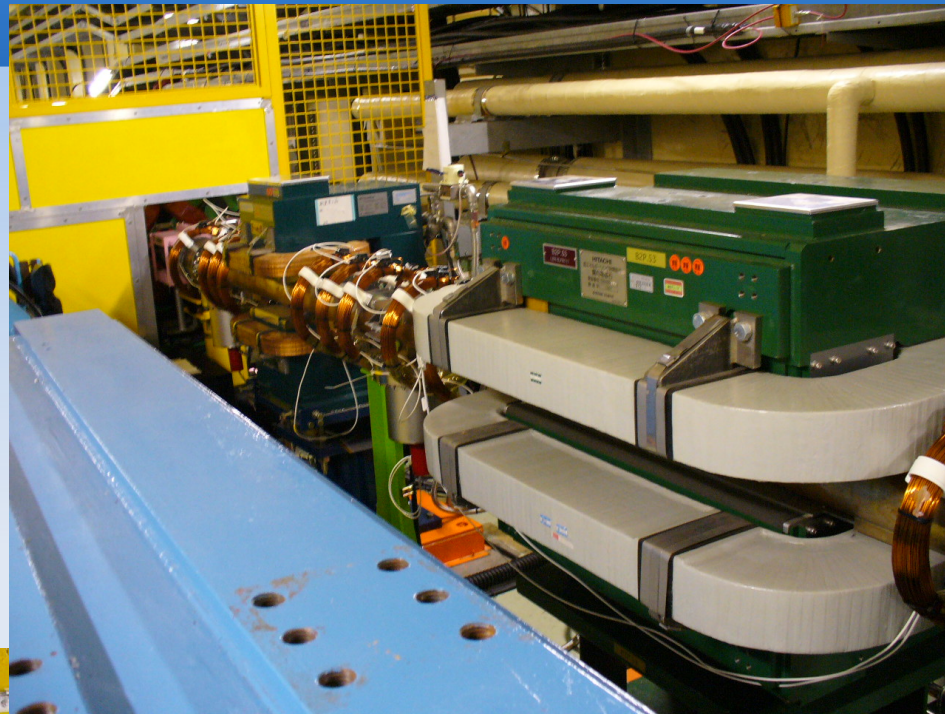
# Energy dependence of attenuation and scattering

- Compton, Rayleigh scattering start to become significant above  $\sim 20$  keV





# X-Ray Source Bend (B2P.53)

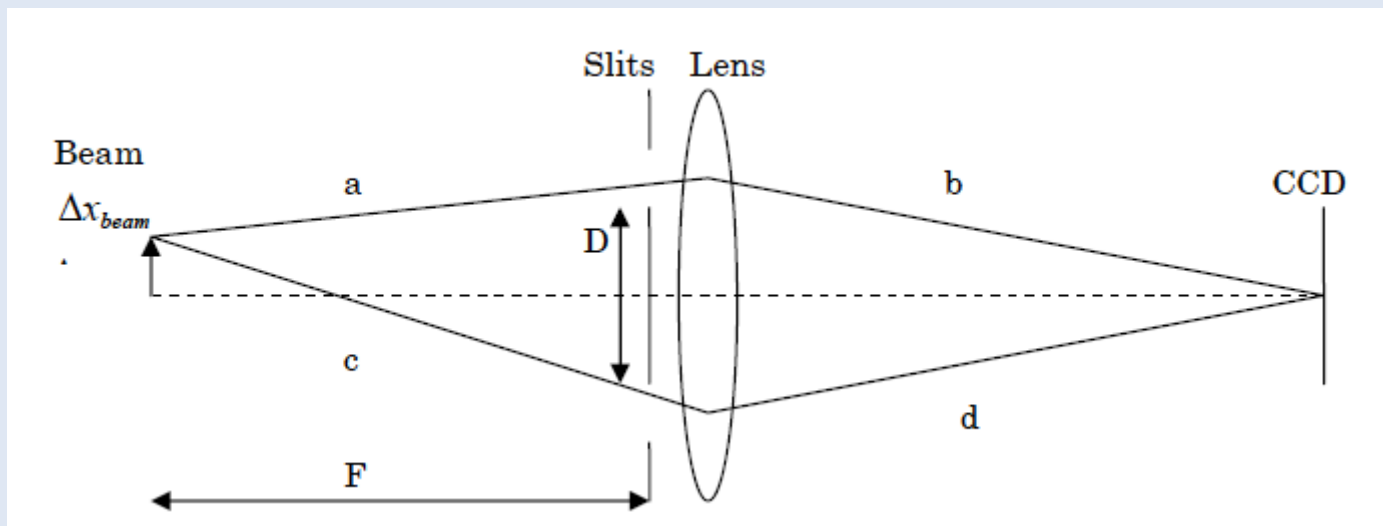


# X-Ray Source & Beamline Parameters

LER B2P.53	KEKB	KEKB-ILCDR	SuperB (LE)
$\epsilon_x$ (m)	1.80E-08	1.50E-09	1.00E-09
$\kappa$ (%)	1%	0.1%	0.1%
$\epsilon_y$ (m)	1.80E-10	1.50E-12	1.00E-12
$\beta_x$ (m)	1.80E+01	1.80E+01	1.80E+01
$\beta_y$ (m)	2.20E+01	2.20E+01	2.20E+01
$\sigma_x$ (m)	5.69E-04	1.64E-04	1.34E-04
$\sigma_y$ (m)	6.29E-05	5.74E-06	4.69E-06
$\sigma_x$ (m)/ $\sigma_y$ (m)	9.05	28.6	28.6
$l$ (a)	2	0.5	8
Bending radius (m)	13.76	13.76	13.76
bend angle (mrad)	56	56	56
Beam Energy (GeV)	3.5	2.3	3.8
kW/mrad/Ampere	0.15	0.15	0.15
Window size (mm)	10	10	10
Window to beam (m)	5	5	5
Power on window (kW)	0.600	0.150	2.400
Power after window (kW)	0.300	0.075	1.200
Mask size (mm)	1	1	1
Beam to mask (m)	6	6	6
Power on mask (kW)	0.025	0.006	0.100
Mask to Detector (m)	24	24	24

# Interferometers

- Beam size at KEKB currently measured by interferometer.
- Resolution fundamentally limited by opening angle between slits from beam.



# Interferometer Source Parameters

LER BWSFRE	KEKB	KEKB-ILCDR	SuperB (LE)
$\varepsilon_x$ (m)	1.80E-08	1.50E-09	1.00E-09
$\kappa$ (%)	1%	0.1%	0.1%
$\varepsilon_y$ (m)	1.80E-10	1.50E-12	1.00E-12
$\beta_x$ (m)	2.42E+01	2.42E+01	2.42E+01
$\beta_y$ (m)	1.77E+01	1.77E+01	1.77E+01
$\sigma_x$ (m)	6.59E-04	1.90E-04	1.55E-04
$\sigma_y$ (m)	5.64E-05	5.15E-06	4.20E-06
$\sigma_x$ (m)/ $\sigma_y$ (m)	11.69	36.97	36.97
I (A)	2	0.5	8
Bending radius $\rho$ (m)	60	60	60
bend angle (mrad)	5	5	5
Beam Energy (GeV)	3.5	2.3	4
Observ. wavelength $\lambda$ (m)	5.00E-07	5.00E-07	5.00E-07
$\omega$ (rad/s)	3.77E+015	3.77E+015	3.77E+015
$\theta_c$ (rad)	0.0016	0.0016	0.0016
Max Slit opening-angle D/F	0.0032	0.0032	0.0032
Max Visibility (fringe modulation) $\gamma$	90%	90%	90%
Minimum measureable beam size $\sigma_{\min}$ (m)	1.15E-05	1.15E-05	1.15E-05

- Note:  $\sigma = \frac{\lambda F}{\pi D} \sqrt{\frac{1}{2} \ln \frac{1}{\gamma}}$        $\frac{D}{F} \leq 2\theta_c$        $\theta_c = \left( \frac{3c}{\omega \rho} \right)^{\frac{1}{3}}$        $\omega = 2\pi \frac{c}{\lambda}$
- D = slit separation, F = distance from beam to slits.
- Max slit opening angle also limited physically with current chamber to ~0.003 rad

# X線テストマスク

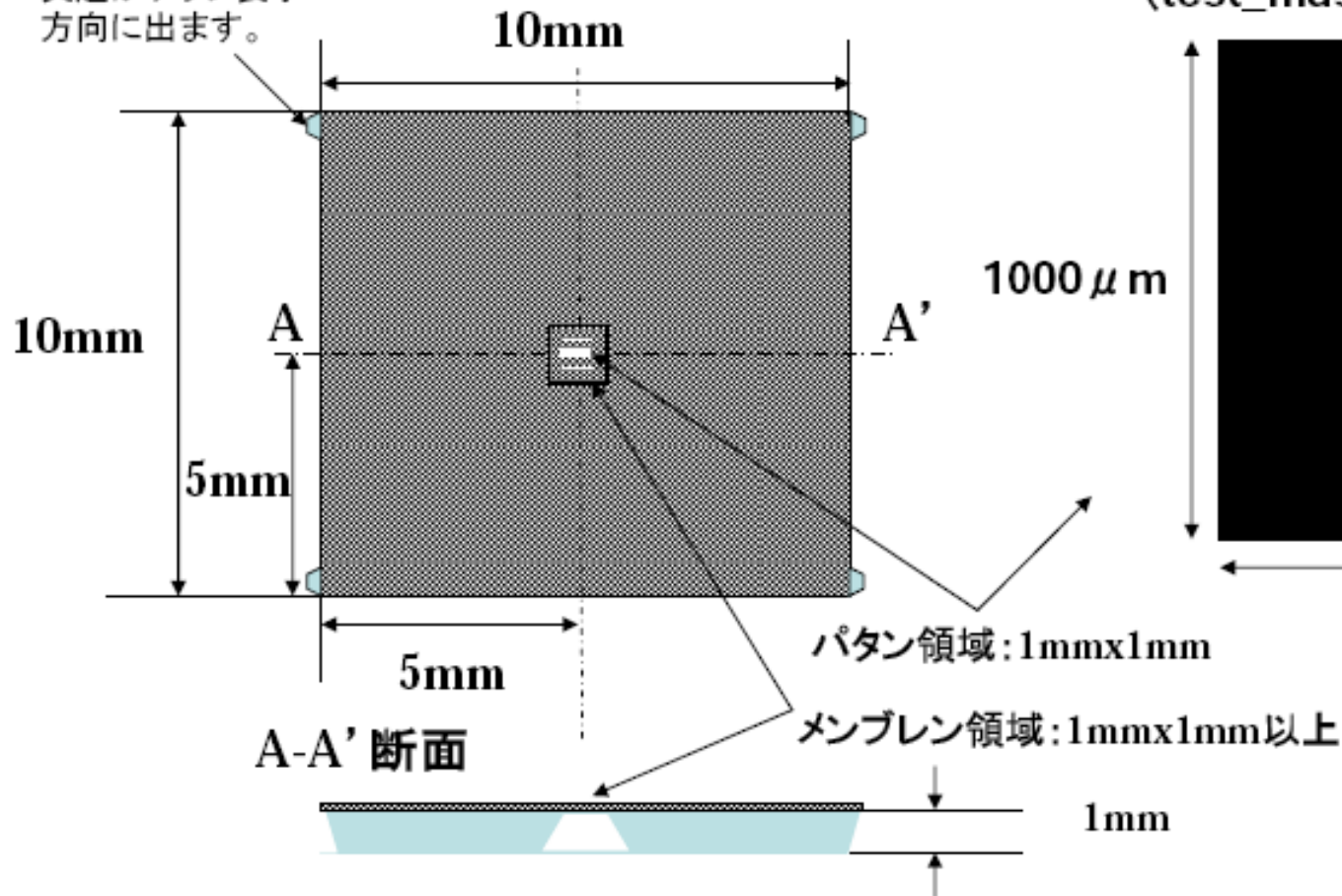
2007.11.20

NTT-ATナノアプリケーション株式会社

ATN仕190424

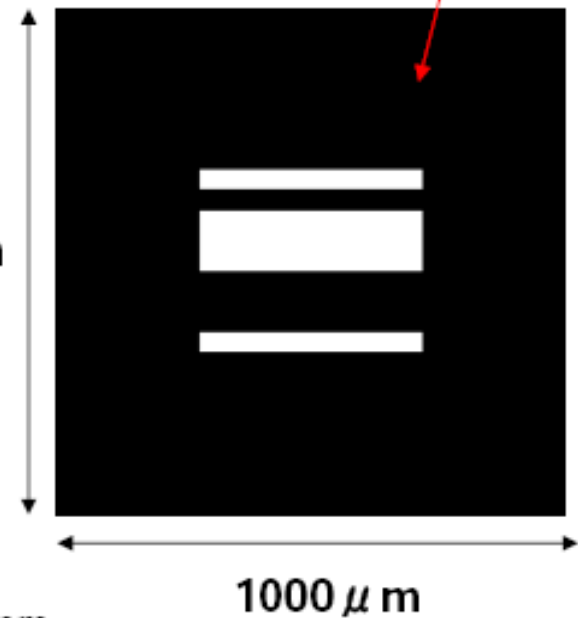
チップ切り出し時に0.5mm程度の突起がチップ長手方向に出ます。

### 基板説明図



### テストマスク (test\_mask1x11)

Ta: 黒部分



基板: Si 10mm角 1mm厚

膜構成: Ta(4 μm)/Ru(0.02 μm)/SiC(1.7 μm)/SiN(0.3 μm)